ABSTRACT

DEMPSEY, LAURA CHANNING LE. A Deep Learning Model for Large Coarse Woody Debris Prediction from Aerial LiDAR on the Malheur National Forest. (Under the direction of Dr. Leah Rathbun).

Traditional field and remote sensing methods have struggled to accurately inventory and model coarse woody debris (CWD) at the small scales required for wildlife habitat management. Percent cover of CWD is mapped across a portion of the Malheur National Forest in eastern Oregon through the integration of aerial laser scanning (ALS) and deep learning (DL). In this novel methodology, the raw LiDAR point cloud is segmented, filtered, and rasterized. Mask R-CNN deep learning object detection is employed on the derived layers to identify individual pieces of CWD and summarize detections into percent cover measurements. These estimates range from 0 % to 10.28 %. The USDA Forest Service PNW Region currently estimates CWD percent cover through a Gradient Nearest Neighbor (GNN) imputation model. The estimates from the DL model are compared against GNN and a set of measured field transects. Limitations of training and validation data hindered full quantification of CWD. However, a large number of successful detections, particularly of larger pieces, demonstrates the potential of this avenue of analysis. This proof of concept study highlights the potential for an ALS and DL based methodology to be integrated into a management platform for Region 6, providing biologists an accurate and higher-resolution tool with which to manage wildlife habitat.

.

A Deep Learning Model for Large Coarse Woody Debris Prediction from Aerial LiDAR on the Malheur National Forest

by
Laura Channing Dempsey

A thesis submitted to the Graduate Faculty of
North Carolina State University
in partial fulfillment of the
requirements for the degree of
Master of Science

Fisheries, Wildlife, and Conservation Biology

Raleigh, North Carolina
2023

APPROVED BY:

_____	_____
Leah Rathbun Committee Chair	Jodi Forrester
_____	Krishna
Pacifici	

DEDICATION

This work is dedicated to my dog Riley for never letting me take myself too seriously and for being the best friend a girl could ask for.

BIOGRAPHY

Laura Dempsey is a life-long lover of wildlife and the natural world. She graduated from Wesleyan University (CT) with a B.A. in Earth and Environmental Science in 2016. She spent the following years working a diverse array of jobs in the federal and private sector. She is passionate about 1) using best available spatial, qualitative, and statistical tools to increase the efficacy of conservation efforts, 2) undertaking research with real-life applications and, 3) promoting effective, cooperative management practices. In her free time, Laura loves skiing, backpacking, and hiking.

ACKNOWLEDGMENTS

I would first and foremost like to think my advisor Dr. Leah Rathbun for her unwavering support over the course of this research. My scientific skills, and more broadly, my capacity for critical thinking, have grown immensely under your instruction and encouragement. Your guidance during such formative stages of my career will doubtless have a life-long impact on my understanding of ecology, and beyond. I am lucky to consider you a mentor.

I am very grateful to the USDA Forest Service for their support of their research. Barbara Garcia was instrumental to the origin of this project. Thank you to Tim Bryant, Jim Muckenhoupt, and Peter Heinzen for providing data and answering numerous questions along the way. Thank you to everyone at the Malheur National Forest. A particularly large dose of gratitude is due to Lauren Romstad, Lori Stokes, and Rachael Vaughn for their hospitality during my field visit.

Thank you to my committee members, Dr. Jodi Forrester, Dr. Krishna Pacifici, and Barbara Garcia, for your time and support. I am also thankful to Dr. Josh Gray who provided guidance about machine learning on several occasions. Thank you to Dr. Ryan Blackburn for being willing to take time out of his busy schedule to discuss all things LiDAR.

Thank you to all my NC pals for the bbqs, tailgates, movie nights, dance parties, rides to the dentist, beach days, and occasional chaos. Thank you to Ben Makhlouf for cheering me up on countless occasions. To Chris, I am so grateful for your constant patience, kindness, and support. Thanks for never doubting that I could do it.

Finally, thank you to my family (Nancy, Guy, Katie, Elizabeth, and Matt). You have always encouraged me to follow my passions, even when they led to unexpected places. I love you guys!

TABLE OF CONTENTS

LIST OF TABLES

LIST OF FIGURES

CHAPTER 1:
Remote Sensing Inventory of Coarse Woody Debris (CWD) Measurement: a review

1. Introduction

Down wood is an essential component of forest ecosystems with extensive ecological benefits. Down wood plays an important role in forest structural diversity, fuel loading, carbon sequestration, nutrient storage and cycling, and wildlife habitat. Specifically in terms of wildlife habitat, down wood provides cover and shelter, creates and maintains microclimates, and provides energy and growth substrate for invertebrates and plants (Bunnell and Houde 2010). Species diversity and abundance, particularly of avian and small mammal species, are positively correlated with the availability of down wood on the landscape (Riffell et al. 2011, Sullivan et al. 2012). Johnson and O'Neil (2018) identified 96 wildlife species, many of which are designated species of concern by federal and state agencies, associated with down wood habitats of the Pacific Northwest. In the Blue Mountains of Oregon and Washington alone, 39 bird and 23 mammal species have been observed nesting and sheltering on large pieces of down wood (Thomas 1979). Coarse woody debris (CWD), also referred to as coarse woody material (CWM), is a catch-all term for larger pieces of down wood. The exact cut-off specifications vary regionally and by institution. The United States Department of Agriculture (USDA) Forest Service (FS) Forest Inventory and Analysis (FIA) protocol defines CWD as down wood greater than or equal to 3 inches in diameter and at least .0.5 feet in length (Forest Inventory and Analysis Program Pacific Northwest Research Station 2022). In practical studies of wildlife habitat, is commonly defined using larger diameter values. Heterogeneous distribution of diverse size classes of CWD across the landscape yields the highest opportunity for wildlife diversity and success; with vertebrates tending to use larger pieces of CWD most often (Butts and McComb 2000). Reliable models and estimates of CWD are critical for responsible management that optimizes the availability of down wood across the landscape.

Distribution of CWD across the landscape is highly variable (Edman and Jonsson 2001). Down wood patterns in Oregon and Washington have shown significant regional variation and were found not to be normally distributed (Waddell and Ohmann 2002, White et al. 2013). In Russian forests, the spatial distribution of CWD pieces of down wood was close to random and did not correlate to other site characteristics (Karjalainen and Kuuluvainen 2002). Attempts to model CWD with other variables such as stand size class, forest type, and land ownership have shown to have poor model fit (R^2=.10) and required prior significant empirical knowledge about the study site in question (Chojnacky and Heath 2002). Ranius et al. (2003) modeled the volume of down wood in Norwegian forests through time using tree growth, tree mortality, and wood decay rates. The model was found to be inaccurate in absence of elements of spontaneous disturbance, illustrating the complexity of modeling these dynamics. The levels

of down wood in an ecosystem are regulated by input through tree mortality or damage and loss through decay or fire consumption. The natural dynamics driving this input depends on several complex factors including successional stage, forest structure, and community composition. Anthropogenic management and disturbance events also contribute CWD to the landscape. CWD is less abundant in managed stands than in unmanaged ones (Green and Peterken 1997, Kirby et al. 1998, Debeljak 2006, Ekbom et al. 2006). Natural boreal spruce forest stands in Sweden had between 10 to 100 times as much CWD as managed stands (Jonsson 2000). Output is regulated by physical characteristics of wood (species and size), local saproxylophagous communities, and climactic factors (Harmon et al. 1986, Hofgaard 1993).

2. Field Measurements of CWD:

An additional complication of this heterogeneity is that accurate field measurements of down wood are onerous to capture. Warren and Olsen introduced line-intersect sampling (LIS) in 1964 as an economic way to assess remaining down wood following logging operations in New Zealand. In this technique, which remains the most common method, any piece of down wood intersecting a straight line is sampled in order to estimate volume (Warren and Olsen 1964). The Brown's transect method of planar intercept was described an extension of LIS to further estimate volume of down wood biomass in order to assess fuel loading (Brown 1971, 1974).

The FIA program collects field information from a plot network across the country in order to assess forest resources. The Pacific Northwest (PNW) region has field plots spaced at intervals of approximately one every 1,800 acres on National Forest System land and incorporated down wood surveys into their inventory during the mid-1980s. They modified the LIS methodology to fit into their existing plot design and framework, although the exact specifications of this transect has been altered through time with adjustments to the FIA field protocols and plot design (Waddell 2002). As of 2022, down wood is measured on transects placed within the 48 ft. diameter FIA subplots (Forest Inventory and Analysis Program Pacific Northwest Research Station 2022).

Measurements from field transects often contain high thresholds of error, the degree of which can be tempered with increased transect numbers and length or through strategic placement through sampling design. However, increasing field efforts caries a substantial monetary and temporal burden. Jordan et al. (2004) found that each piece of wood in a LIS takes on average 90 seconds, to inventory although topography can drastically increase this duration. CWD pieces with high levels of decay or irregular shapes can prove particularly difficult to accurately inventory in the field (Campbell et al. 2019). In terms of transect length, Woldendorp et al. (2004)suggests high intensity sampling is required for volume estimates with a coefficient of variation less than 0.5; dense forests could require transects over 320 ft long to achieve high accuracy of any volume. A more attainable option is often to focus on strategic

placement of plots across the landscape which can reduce the overall quantity of transects needed to collect representative data (Pesonen et al. 2010).

Double-sampling for stratification is a two-step methodology used in forest inventories when the area of interest is too large to stratify in its entirety. In the initial step, a large sample is taken and classified using remote imagery. This information is used to estimate the weights of each stratum. In phase two, subsamples are drawn by strata from the initial group; the weight estimate for each group is included in the variance (Cochran 1997, Scott 1998). Since the 1950s, FIA has used double sampling for stratification in a three-phase approach. Initially, in phase one, imagery is used to classify a large sample of plots into different land cover classes. In phase two, crews systemically select a subset of those points across different strata to install field plots. Finally, a subset of field plots are selected as phase three plots where additional information, including data on CWD transects, are collected. Aerial photos were initially used as the basis of FIA stratification. However, the required manual ocular, interpretation of aerial photographs, or photointerpretation, is time consuming and can be biased and inaccurate. Other hurdles of photointerpretation include the cost and difficulty of acquiring high quality photos, physical storage needs of large photo collections, and lack of unbiased interpreters who are often familiar with the areas (Hansen 2001, Chojnacky and Heath 2002, Kaartinen et al. 2002). Remote sensing technology and digital mapping software can automate much of this stratification process.

3. Remote Sensing Measurements of CWD

Stratification based on remotely sensed imagery is less expensive and has comparable precision to manual photointerpretation (Kaartinen et al. 2002). Stratum derived using national agriculture imagery program (NAIP) aerial digital photography from 2015 consistently outperformed those created from manual photointerpretation (Westfall et al. 2019). As access to satellite imagery increased across the country, satellite based classifications, particularly two-dimensional LANDSAT imagery, began to supersede photos as the backbone of FIA's double sampling (Roesch and Moisen 2005). Despite the complexity of CWD dynamics, studies have shown these patterns tend to vary by forest type (Siitonen et al. 2000, Pedlar et al. 2002, Lombardi et al. 2008, Oettel et al. 2020). In Oregon and Washington the volume of CWD (≥ 50.0 cm large end diameter and ≥ 2.0 m length) was largest in westside conifer-forests (131.8 mean cubic meters per hectare) and smallest in western juniper woodlands (4.5 mean cubic meters per hectare) (Waddell and Ohmann 2002). Stratification by variables such as land cover and forest type can thereby increase accuracy of CWD estimates (Woldendorp et al. 2002).

Another method to integrate field data and remote sensing is imputation modeling. Statistical imputation is a process that populates missing or new values using existing values based on developing criteria from additional data (e.g. location or satellite imagery). One such technique, nearest-neighbor (NN) modelling, is common in forestry and ecological monitoring where remote sensing data is available

for the entire population as an explanatory variable, but field data, or the response variables, has been collected only on smaller subset of areas. Ohmann and Gregory (2002) created gradient nearest neighbor (GNN) imputation mapping as synthesis of direct gradient analysis and imputation mapping (Gauch 1982). Thus, a donor pixel containing field-measured data is used to fill in information about vegetation structure in a pixel without field data so long as the pixels are similar and physically nearby. This GNN methodology creates the basis through which the Forest Service Pacific Northwest Region 6 (R6) currently models and manages down wood in the PNW. This mapping effort, through Oregon State University, is central to central to the Decayed Wood Advisor (DecAID) platform: a management tool that catalogs down wood conditions for reference and current conditions and describes wildlife habitat on federally managed lands in the PNW. Although DecAID is a powerful management tool, it is most robust at broader spatial scales and even then, the accuracy varies. There remains a need for better estimates of CWD at smaller scales such as at the project or stand-level. LANDSAT imagery currently comprises the explanatory variable for that sampling frameworks (Ohmann and Gregory 2002).

Time series of LANDSAT imagery has additionally been used to assess CWD in conifer forests in western North America through the compilation of change detection algorithms, aerial forest health detection surveys, and LIS on field plots to assess how spectral changes correspond with changes in amount of CWD. These spectral changes were found to be related to the cover of CWD ($R^2adj = 0.29$, $F_1 = 14.72$, $P = 0.0006$)(Meigs et al. 2011).

Active sensor technology like aerial laser scanning (ALS), also known as plane mounted LiDAR sensors, offer the potential to capture forest structure metrics on smaller scales with increased accuracy compared to methods that use satellite imagery alone (Zald et al. 2014, Zald et al. 2016). Unlike passive sensors that reflect energy from the sun, such as LANDSAT, active sensors generate their own energy and can provide information on the elevation profile through analyzing the return time intervals (Magnussen and Boudewyn 1998, Dubayah and Drake 2000). This sensor technology is utilized in forestry through a range of platforms including terrestrial laser scanning (TLS) and airborne laser scanning (ALS). TLS produces extremely high- resolution data but is not widely available or appropriate for use over a large area due to physical constraints (Danson et al. 2018). ALS is a practical compromise for forestry management between resolution and spatial extent as large areas can be covered by either plane, helicopter, or unmanned aerial vehicle (UAV). Additionally, increases in ALS sensor technology have increased the resolution of data while simultaneously reducing costs of acquisition. The past decades have seen a proliferation of ALS used for measurements and estimates of forest characteristics. Previous work has shown ALS derived maps offer increased accuracy to passive multispectral sensors like LANDSAT (Zald et al. 2014).

ALS data can be used to study a multitude of forest characteristics such as basal area (Maltamo et al. 2007), stem diameter (Shang et al. 2017), stand volume (Packalén and Maltamo 2007), stand density (Montealegre et al. 2016), tree height (Wang et al. 2019), crown metrics (Pyörälä et al. 2019) and biomass (Næsset and Gobakken 2008, Nelson et al. 2017). Initial studies tended to focus on canopy metrics (White et al. 2013) as upper layers of canopy limit the number of ALS pulses that reach the forest floor, adding an additional element of complexity to isolating understory metrics, like down wood, from these airborne measurements (Hill et al. 2009). Forest type, shrub density and canopy cover affect the severity of this occlusion (Morsdorf et al. 2010, Crespo-Peremarch et al. 2020). Some studies approached the topic of dead wood in the forest ecosystem by using ALS to measure standing dead trees, often referred to as snags. (Bater et al. 2007, Casas et al. 2016). Increases in sensor technology and analysis technique began to open the way for more fine-scale analysis of understory metrics.

4. ALS Measurements of CWD

The earliest studies integrating ALS to assess CWD tended to use a more indirect area-based approach. Seielstad and Queen (2003) used ALS data to create generalized fuel models on the landscape scale but with the suggestion that more direct measurements of CWD may soon be feasible. Pesonen et al. (2008) explored the potential of ALS to estimate the volume of CWD in Finland in 2008. They looked at the relationship between characteristics of the ALS point cloud like heights of first and last pulse and derived forest metrics such as height with CWD volume (R^2=0.61, RMSE 52.6%.) They found that the remote sensing-based estimates of down wood volume had increased accuracy when compared to volume estimates based on field-measurements of live trees. Van Aardt et al. (2011) further correlated LiDAR height distributions and scattering patterns with CWD to estimate fuel loading in oak forests in Kentucky.

Another avenue of research is the more direct analysis of LiDAR-derived raster layers. Lindberg et al. (2013) applied a line template matching algorithm directly to the near ground returns from an ALS point cloud in Sweden. The results of this matching are rasterized into a layer representing the level of confidence for each linear detection and the lines themselves overlaid as vectors. The model detected 854 total lines; 268 of these were automatically validated through field measurements of a total of 651 large pieces of down wood. Complex arrangement of pieces such as found following disturbance, understory vegetation, and linear ground features such as ditches and roads resulted in lower detection certainty (Lindberg et al. 2013). Nyström (2014) looked at the height variation between two ALS derived elevation models (active surface DEM and ground DEM) from Northern Sweden and applied a line matching template to the resulting map of differences. From this, individual large wind thrown trees on the landscape could be detected; 38% of wind thrown trees were detected although tree diameter and length played a significant role in detection. Understory vegetation and ground features like ditches further complicated overall accuracy. Multitemporal ALS datasets were also used to identify changes or additions

to the down wood volume between two time periods (Næsset 2002). Lopes Queiroz et al. (2020) derived optical imagery and vegetation index layers from multi-spectrum ALS in Alberta, Canada in order to predict CWD (R^2=0.62). Mücke (2013) used discrete ALS data to create modified raster layers of the earth's surface and derived measures of surface roughness from which they manually extracted linear CWD features; identifying 77.8% of the CWD in the study area. Shokirov et al. (2021) also derived raster layers of surface characteristics from high-resolution multiplatform LiDAR but used an automated Random Forest (RF) Machine Learning (ML) method to identify pixels associated with CWD. Through this exercise they found surface roughness, a measure of the largest inter-cell difference of a focal cell and its 8 neighboring pixels, to be the most significant variable for CWD identification (Amatulli et al. 2018).

Direct analysis of the point cloud can also identify individual CWD pieces. Segmentation of the point cloud based on height metrics allows researchers to isolate CWD objects for analysis. Joyce et al. (2019) used height cut-offs of 0 and 130 cm to vertically segment the point cloud and manually identify CWD objects within the truncated portions. Overall, 23% of individual CWD pieces mapped in the field were detected. Larger pieces were easier to detect; most detected logs were larger than 30 cm in diameter and 13.9 meters long. Jarron et al. (2021) isolated CWD objects (> 30 cm in diameter) from the point cloud though a process of grounding algorithms, height segmentation, filtering, and linear pattern recognition. This transformed the point cloud into vectorized shapes that could be validated against field measurements. 64% of individual pieces and 79% of CWD volume within plots was detected. High levels of decay negatively impacted detection.

5. ALS Characteristics and CWD

ALS characteristics including intensity, return number, and pulse density can be used to overcome a handful obstacles complicating ALS CWD measurements. Intensity is the power of the returned laser light per unit area. A single emitted ALS pulse can refract and divide when it hits various features. Both return number and number of returns reflect this characteristic. Finally, pulse density is the number of pulses sent by the sensor per square meter (pulses m−2). Higher pulse densities are more expensive to collect although improvements to technology are reducing that economic obstacle (Béland et al. 2014).

Understory vegetation and ground features were commonly cited as impediments to ALS based measurements of understory metrics like CWD, particularly when taken during leaf-on conditions (Lindberg et al. 2013, Nyström 2014). Filtering data based on different intensity metrics can provide more accurate measurements of biomass (Lim et al. 2003, Kim et al. 2009). The identification of characteristic intensity and return profiles for understory vegetation allows the creation of filters that remove such objects from the point cloud, allowing further isolation of the points of interest (Wing et al. 2012).

LiDAR pulses that pass through complex structures of twigs or shrubs are more likely to come back as multiple returns, compared to pulses that hit the ground or singular objects unimpeded (Raber et

al. 2002). One study found that that 81% (SD: 10%) of multiple returns during leaf-on collection relate to partial hits on branches, deciduous leaves, or twigs (Béland et al. 2014). As such, multiple returns near the ground can logically assumed to be associated with shrubs or understory vegetation as opposed to CWD (Jarron et al. 2021)

Higher pulse density means that more information is being collected. Ground and understory density are also critical in that they reflect the amount of information reaching the CWD objects of interest. This sensitivity was quantified by Joyce et al. (2019) who identified a critical pulse density of > 7 pls/m^2 at which point CWD detection surpassed 50%.

6. Object-Based Image Analysis

When an ALS point cloud is "rasterized', as is commonly required at some point in many analyses, the information is rendered into a two-dimensional grid of pixels with information stored within each cell. Early remote sensing projects often relied on pixel by pixel classification that failed to capture the larger spatial relationships within data (Blaschke 2010). In object-based image analysis (OBIA), homogenous groups of pixels are grouped together through image classification and extracted and analyzed in meaningful groups rather than as individuals (Blaschke 2010, Hossain and Chen 2019). Although the initial segmentation and classification parameters can be complex, OBIA has higher classification accuracy than single-pixel approaches and can capture details (such as texture and shape) that would otherwise be inaccessible (Blanchard et al. 2011).

In forestry, OBIA had been used with passive sensor technology, like LANDSAT, to map forest types and track forest change (Flanders et al. 2003, De Chant and Kelly 2009). Sullivan et al. (2009) used OBIA with ALS-derived maps of canopy to delineate stand maps in western Oregon with accuracy rates between 78 and 84%. In 2011, Blanchard et al. (2011) used OBIA with a ALS derived raster layer to identify 73% of pieces of down wood (defined by small end diameter greater than or equal to 9.8 inches and a minimum length greater than or equal to 16.4 feet) in California. Over classification was problematic in areas with high density of logs or thick understory vegetation. The authors deemed the technique effective but inefficient as the segmentation and classification required significant time inputs from human analysis and interpretation.

A consequence of increased data collection ability in both resolution and scope is the need for more streamlined and automated processing and analysis. Krisanski et al. (2021) found that automated segmentation and classification of the forest understory through density-based spatial clustering of applications with noise (DBSCAN) unsupervised classification of merged terrestrial laser scanning (TLS) and ALS data sets achieved 54.98% accuracy in identifying coarse down wood with extremely high resolution input data. Windrim et al. (2019) automated volume estimates of CWD from high-resolution drone-based LiDAR on a post-harvest pine plantation using automated detection and segmentation.

7. Deep Learning and CWD

In deep learning, a specific subset of machine learning, a computer relies on a series of processing units called neural networks. These adaptive networks learn using interconnected nodes that resemble the structure of a human brain. While traditional neural networks might contain one or two layers, the neural networks in deep learning stack hidden layers together to increase the leaning potential to understand complex patterns (Goodfellow et al. 2016). While multiple types of these networks exist, convolutional neural network (CNNs) are particular adept at issues of imagery identification and classification (LeCun et al. 2015, Borowiec et al. 2022). In the convolutional layer of a CNN, a feature detector (often called a kernel or filter), moves across the input image to ascertain if the feature of interest is present (Albawi et al. 2017). CNNs are trained to learn the spatial features or characteristics that define the objects in question and are particularly well suited to vegetation analysis although much of this research is novel or on-going.

Deep learning overcomes many of the previous manual inefficiencies associated with machine learning detection of CWD. A literature review of studies using CNN-based vegetation studies found a total of 101 studies published on the topic. 75% of the studies were published in or after 2019 and none were from before 2016. In 2020, more than 50% of these studies to date were based on TLS or LiDAR data from UAVs, likely related to the increased resolution and point density of these data collections method. Less than 5 studies had been conducted using ALS data (Kattenborn et al. 2021). These metrics underscore how novel this area of research is.

Safonova et al. (2019) used a two-stage approach of deep learning with UAV LiDAR data to identify fir trees (*Abies sibirica*) damaged by bark beetles in Russia. They trained a CNN model with six convolutional blocks that can recognize four different damage categories in Siberian firs. Their model showed an accuracy rating of over 98% for three of the four classes. Thiel et al. (2020) analyzed UAV LiDAR data with a deep learning framework combined with a line matching algorithm approach to assess CWD in an area in Germany. 75% of CWD objects were detected although this methodology is more suited for fine scale analysis over a smaller area following a known disturbance or management event.

Until quite recently, DL has not been applied to ALS based CWD quantification, particularly not at the project area or landscape level scale. Region based CNNs are perhaps the most common object detection methodology in vegetation studies. In this methodology, a region of interest is identified and then an object is detected within. Mask Region Based CNN (Mask R-CNN) is a novel methodology in deep learning that detects and segments objects from an image with high accuracy and requires little input from the user beyond initial training samples (He et al. 2017). Dempsey and Rathbun (2022) mapped the percent cover of CWD on a national forest in Oregon using deep learning. A strategically filtered ALS point cloud was rasterized into a multi-band layer of elevation profiles from which Mask R-CNN object

detection deep learning could detect individual pieces of wood. These pieces were measured and summarized as percent cover although an absence of a rigorous training data set limited studies' validation and scope.

ESRI's ArcGIS Image Analyst extension allows geospatial based deep learning workflows to be performed wholly within ArcGIS pro (Bennett 2018). ENVI deep learning module extension (*Exelis Visual Information Solutions, Boulder, Colorado*) provides an intuitive platform for imagery based deep learning without the need for any specific programming skills (Glatz and Bahr 2018). These tool and similar types of integrated workflows remove some of the previously prohibitive technical barriers to deep learning, such as fluency in python script.

8. Data Limitations

Deep learning is best suited for large, balanced data sets. Unfortunately, in practical applications to ecology, this is rarely the case. Data sets from the natural world are often sparse, skewed, and imbalanced Classes with more samples are given higher weight by the model (Villon et al. 2022). Data augmentation can be used to combat this imbalance and inflate the number of samples in the underrepresented class to increase their weight in model learning. This can be achieved in multiple ways including resampling, geometric transformation, or feature space augmentation (Van Dyk and Meng 2001, Shorten and Khoshgoftaar 2019). Additionally, the object of interest in ecology is often rare or underrepresented in the dataset, thereby making it difficult to pull a sufficient set of training data. Few-shot learning (FSL) is a developing field that can tackle classification problems with only a limited number of training samples (Fink 2004, Villon et al. 2021). FSL has been applied in remote sensing studies of image classification (Chen et al. 2021, Pal et al. 2022), object recognition (Antonelli et al. 2022) , and object detection (Fei-Fei et al. 2006, Hong et al. 2022). Karami et al. (2020) applied FSL techniques with RGB UAV images to identify and tally maize plants but found the accuracy lagged behind more traditional deep learning. Wei et al. (2022) mapped a large area of forest in China with FLS and high-resolution satellite imagery; they propose an FSL technique requiring limited ground-truthing data but high accuracy (F1=84.23%). Sun et al. (2021) tracked the publication of FSL research for remote sensing interpretation from 2009 to 2019 from 3 to 64 studies. Despite the increasing interest and investment in this area of research, they conclude the field is still in its infancy. FSL has not yet been applied to any published analysis of understory metrics or CWD.

9. Future Study

As these methods develop, so expands the possibilities of research question. Priority areas for future study are suggested as:

- Deep learning analysis of ALS data with more rigorous training and validation data sets
- Application of data augmentation methods to balance out issues of CWD sample scarcity

- Application of few-shot learning methodology
- The development of deep learning algorithms better suited to forestry rather than adapted from other sectors
- Exploration of ALS characteristics like intensity to potential reflect metrics such as decay class
- Creation of maps of wildlife habitat suitability based on CWD metrics
- Mapping of wildlife travel or dispersal corridors based on information about orientation and distribution of individual pieces of wood

10. Conclusion:

Remote sensing has revolutionized the field of CWD measurement. Advanced sensor technology and high resolution optics facilitated the collection of understory data that was previously occluded from aerial observation. Advancements in the understanding of CWD characteristics and filtering techniques enabled CWD objects to be more easily isolated. The fields of machine learning and deep learning further advanced the field's ability to process large data sets, often autonomously. The advancements in the field of CWD measurement are moving in a promising direction to facilitate the arrival of fine-scale models with the hope that land managers can use these tools to manage wildlife habitat even for species with highly-specific niches.

REFERENCES

Aardt, J. v., M. A. Arthur, G. Sovkoplas, and T. L. Swetnam. 2011. LiDAR-based estimation of forest floor fuel loads using a novel distributional approach.

Albawi, S., T. A. Mohammed, and S. Al-Zawi. 2017. Understanding of a convolutional neural network. Pages 1-6 *in* 2017 international conference on engineering and technology (ICET). Ieee.

Amatulli, G., S. Domisch, M.-N. Tuanmu, B. Parmentier, A. Ranipeta, J. Malczyk, and W. Jetz. 2018. A suite of global, cross-scale topographic variables for environmental and biodiversity modeling. Scientific data **5**:1-15.

Antonelli, S., D. Avola, L. Cinque, D. Crisostomi, G. L. Foresti, F. Galasso, M. R. Marini, A. Mecca, and D. Pannone. 2022. Few-shot object detection: A survey. ACM Computing Surveys (CSUR) **54**:1-37.

Bater, C., N. Coops, S. Gergel, and N. Goodwin. 2007. Towards the estimation of tree structural class in northwest coastal forests using lidar remote sensing.

Béland, M., D. D. Baldocchi, J.-L. Widlowski, R. A. Fournier, and M. M. Verstraete. 2014. On seeing the wood from the leaves and the role of voxel size in determining leaf area distribution of forests with terrestrial LiDAR. Agricultural and Forest Meteorology **184**:82-97.

Bennett, L. 2018. Machine learning in ArcGIS. ArcUser **21**:8-9.

Blanchard, S. D., M. K. Jakubowski, and M. Kelly. 2011. Object-Based Image Analysis of Downed Logs in Disturbed Forested Landscapes Using Lidar. Remote Sensing **3**:2420-2439.

Blaschke, T. 2010. Object based image analysis for remote sensing. ISPRS Journal of Photogrammetry and Remote Sensing **65**:2-16.

Borowiec, M. L., R. B. Dikow, P. B. Frandsen, A. McKeeken, G. Valentini, and A. E. White. 2022. Deep learning as a tool for ecology and evolution. Methods in Ecology and Evolution **13**:1640-1660.

Brown, J. K. 1971. A Planar Intersect Method for Sampling Fuel Volume and Surface Area. Forest Science **17**:96-102.

Brown, J. K. 1974. Handbook for inventorying downed woody material.

Bunnell, F. L., and I. Houde. 2010. Down wood and biodiversity — implications to forest practices. Environmental Reviews **18**:397-421.

Butts, S. R., and W. C. McComb. 2000. Associations of Forest-Floor Vertebrates with Coarse Woody Debris in Managed Forests of Western Oregon. The Journal of Wildlife Management **64**:95-104.

Campbell, J. L., M. B. Green, R. D. Yanai, C. W. Woodall, S. Fraver, M. E. Harmon, M. A. Hatfield, C. J. Barnett, C. R. See, and G. M. Domke. 2019. Estimating uncertainty in the volume and carbon storage of downed coarse woody debris. Ecological Applications **29**:e01844.

Casas, Á., M. García, R. B. Siegel, A. Koltunov, C. Ramírez, and S. Ustin. 2016. Burned forest characterization at single-tree level with airborne laser scanning for assessing wildlife habitat. Remote Sensing of Environment **175**:231-241.

Chen, L., X. Tian, G. Chai, X. Zhang, and E. Chen. 2021. A new CBAM-P-Net model for few-shot forest species classification using airborne hyperspectral images. Remote Sensing **13**:1269.

Chojnacky, D. C., and L. S. Heath. 2002. Estimating down deadwood from FIA forest inventory variables in Maine. Environmental Pollution **116**:S25-S30.

Cochran, W. 1997. Sampling Techniques. 3 edition. Wiley.

Crespo-Peremarch, P., R. A. Fournier, V.-T. Nguyen, O. R. van Lier, and L. Á. Ruiz. 2020. A comparative assessment of the vertical distribution of forest components using full-waveform airborne, discrete airborne and discrete terrestrial laser scanning data. Forest Ecology and Management **473**:118268.

Danson, F. M., M. I. Disney, R. Gaulton, C. Schaaf, and A. Strahler. 2018. The terrestrial laser scanning revolution in forest ecology. Page 20180001. The Royal Society.

De Chant, T., and M. Kelly. 2009. Individual object change detection for monitoring the impact of a forest pathogen on a hardwood forest. Photogrammetric Engineering & Remote Sensing **75**:1005-1013.

Debeljak, M. 2006. Coarse woody debris in virgin and managed forest. Ecological Indicators **6**:733-742.

Dubayah, R. O., and J. B. Drake. 2000. Lidar remote sensing for forestry. Journal of Forestry **98**:44-46.

Edman, M., and B. G. Jonsson. 2001. Spatial pattern of downed logs and wood-decaying fungi in an old-growth Picea abies forest. Journal of Vegetation Science **12**:609-620.

Ekbom, B., L. M. Schroeder, and S. Larsson. 2006. Stand specific occurrence of coarse woody debris in a managed boreal forest landscape in central Sweden. Forest Ecology and Management **221**:2-12.

Fei-Fei, L., R. Fergus, and P. Perona. 2006. One-shot learning of object categories. IEEE transactions on pattern analysis and machine intelligence **28**:594-611.

Fink, M. 2004. Object classification from a single example utilizing class relevance metrics. Advances in neural information processing systems **17**.

Flanders, D., M. Hall-Beyer, and J. Pereverzoff. 2003. Preliminary evaluation of eCognition object-based software for cut block delineation and feature extraction. Canadian Journal of Remote Sensing **29**:441-452.

Forest Inventory and Analysis Program Pacific Northwest Research Station. 2022. Field Instructions for the Annual Inventory of California, Oregon, and Washington 2022. USDA Forest Service.

Gauch, H. G. 1982. Multivariate Analysis in Community Ecology. Cambridge University Press, Cambridge.

Glatz, W., and T. Bahr. 2018. A Service Architecture for Processing Big Earth Data in the Cloud with Geospatial Analytics and Machine Learning.

Goodfellow, I., Y. Bengio, and A. Courville. 2016. Deep learning. MIT press.

Green, P., and G. Peterken. 1997. Variation in the amount of dead wood in the woodlands of the Lower Wye Valley, UK in relation to the intensity of management. Forest Ecology and Management **98**:229-238.

Hansen, M. H. 2001. Remote Sensing Precision Requirements For FIA Estimation.

Harmon, M. E., J. F. Franklin, F. J. Swanson, P. Sollins, S. Gregory, J. Lattin, N. Anderson, S. Cline, N. Aumen, and J. Sedell. 1986. Ecology of coarse woody debris in temperate ecosystems. Advances in ecological research **15**:133-302.

He, K., G. Gkioxari, P. Dollár, and R. Girshick. 2017. Mask r-cnn. Pages 2961-2969 *in* Proceedings of the IEEE international conference on computer vision.

Hill, R. A., S. A. Hinsley, and R. K. Broughton. 2009. Assessing habitats and organism-habitat relationships by ALS 2.

Hofgaard, A. 1993. 50 years of change in a Swedish boreal old-growth Picea abies forest. Journal of Vegetation Science **4**:773-782.

Hong, B., Y. Zhou, H. Qin, Z. Wei, H. Liu, and Y. Yang. 2022. Few-Shot Object Detection Using Multimodal Sensor Systems of Unmanned Surface Vehicles. Sensors **22**:1511.

Hossain, M. D., and D. Chen. 2019. Segmentation for Object-Based Image Analysis (OBIA): A review of algorithms and challenges from remote sensing perspective. ISPRS Journal of Photogrammetry and Remote Sensing **150**:115-134.

Jarron, L. R., N. C. Coops, W. H. MacKenzie, and P. Dykstra. 2021. Detection and Quantification of Coarse Woody Debris in Natural Forest Stands Using Airborne LiDAR. Forest Science **67**:550-563.

Johnson, D. H., and T. O'Neil. 2018. Wildlife Habitat Relationships in Oregon and Washington. Oregon State University Press.

Jonsson, B. G. 2000. Availability of coarse woody debris in a boreal old-growth Picea abies forest. Journal of Vegetation Science **11**:51-56.

Jordan, G. J., M. J. Ducey, and J. H. Gove. 2004. Comparing line-intersect, fixed-area, and point relascope sampling for dead and downed coarse woody material in a managed northern hardwood forest. Canadian Journal of Forest Research **34**:1766-1775.

Joyce, M. J., J. D. Erb, B. A. Sampson, and R. A. Moen. 2019. Detection of coarse woody debris using airborne light detection and ranging (LiDAR). Forest Ecology and Management **433**:678-689.

Kaartinen, A. T., J. S. Fried, and P. A. Dunham. 2002. Efficiency and precision for estimating timber and non-timber attributes using Landsat-based stratification methods in two-phase sampling in northwest California.*in* In: McRoberts, Ronald E.; Reams, Gregory A.; Van Deusen, Paul C.; Moser, John W., eds. Proceedings of the Thrid Annual Forest Inventory and Analysis Symposium; Gen. Tech. Rep. NC-230. St. Paul, MN: US Department of Agriculture, Forest Service, North Central Research Station: 69-79.

Karami, A., M. Crawford, and E. J. Delp. 2020. Automatic Plant Counting and Location Based on a Few-Shot Learning Technique. IEEE Journal of Selected Topics in Applied Earth Observations and Remote Sensing **13**:5872-5886.

Karjalainen, L., and T. Kuuluvainen. 2002. Amount and diversity of coarse woody debris within a boreal forest landscape dominated by Pinus sylvestris in Vienansalo wilderness, eastern Fennoscandia. Silva Fennica **36**:147-167.

Kattenborn, T., J. Leitloff, F. Schiefer, and S. Hinz. 2021. Review on Convolutional Neural Networks (CNN) in vegetation remote sensing. ISPRS Journal of Photogrammetry and Remote Sensing **173**:24-49.

Kim, Y., Z. Yang, W. B. Cohen, D. Pflugmacher, C. L. Lauver, and J. L. Vankat. 2009. Distinguishing between live and dead standing tree biomass on the North Rim of Grand Canyon National Park, USA using small-footprint lidar data. Remote Sensing of Environment **113**:2499-2510.

Kirby, K., C. Reid, R. Thomas, and F. Goldsmith. 1998. Preliminary estimates of fallen dead wood and standing dead trees in managed and unmanaged forests in Britain. Journal of applied ecology **35**:148-155.

Krisanski, S., M. S. Taskhiri, S. Gonzalez Aracil, D. Herries, and P. Turner. 2021. Sensor Agnostic Semantic Segmentation of Structurally Diverse and Complex Forest Point Clouds Using Deep Learning. Remote Sensing **13**:1413.

LeCun, Y., Y. Bengio, and G. Hinton. 2015. Deep learning. nature **521**:436-444.

Lim, K., P. Treitz, K. Baldwin, I. Morrison, and J. Green. 2003. Lidar remote sensing of biophysical properties of tolerant northern hardwood forests. Canadian Journal of Remote Sensing **29**:658-678.

Lindberg, E., M. Hollaus, W. Mücke, J. Fransson, and N. Pfeifer. 2013. Detection of lying tree stems from airborne laser scanning data using a line template matching algorithm.

Lombardi, F., B. Lasserre, R. Tognetti, and M. Marchetti. 2008. Deadwood in relation to stand management and forest type in Central Apennines (Molise, Italy). Ecosystems **11**:882-894.

Lopes Queiroz, G., G. J. McDermid, J. Linke, C. Hopkinson, and J. Kariyeva. 2020. Estimating Coarse Woody Debris Volume Using Image Analysis and Multispectral LiDAR. Forests **11**:141.

Magnussen, S., and P. Boudewyn. 1998. Derivations of stand heights from airborne laser scanner data with canopy-based quantile estimators. Canadian Journal of Forest Research **28**:1016-1031.

Maltamo, M., A. Suvanto, and P. Packalén. 2007. Comparison of basal area and stem frequency diameter distribution modelling using airborne laser scanner data and calibration estimation. Forest Ecology and Management **247**:26-34.

Meigs, G. W., R. E. Kennedy, and W. B. Cohen. 2011. A Landsat time series approach to characterize bark beetle and defoliator impacts on tree mortality and surface fuels in conifer forests. Remote Sensing of Environment **115**:3707-3718.

Montealegre, A. L., M. T. Lamelas, J. de la Riva, A. García-Martín, and F. Escribano. 2016. Use of low point density ALS data to estimate stand-level structural variables in Mediterranean Aleppo pine forest. Forestry: An International Journal of Forest Research **89**:373-382.

Morsdorf, F., A. Mårell, B. Koetz, N. Cassagne, F. Pimont, E. Rigolot, and B. Allgöwer. 2010. Discrimination of vegetation strata in a multi-layered Mediterranean forest ecosystem using height and intensity information derived from airborne laser scanning. Remote Sensing of Environment **114**:1403-1415.

Mücke, W. 2013. Comparison of discrete and full-waveform ALS for dead wood detection.

Næsset, E. 2002. Predicting forest stand characteristics with airborne scanning laser using a practical two-stage procedure and field data. Remote Sensing of Environment **80**:88-99.

Næsset, E., and T. Gobakken. 2008. Estimation of above- and below-ground biomass across regions of the boreal forest zone using airborne laser. Remote Sensing of Environment **112**:3079-3090.

Nelson, R., H. Margolis, P. Montesano, G. Sun, B. Cook, L. Corp, H.-E. Andersen, B. deJong, F. P. Pellat, T. Fickel, J. Kauffman, and S. Prisley. 2017. Lidar-based estimates of aboveground biomass in the continental US and Mexico using ground, airborne, and satellite observations. Remote Sensing of Environment **188**:127-140.

Nyström, M. 2014. Mapping and monitoring of vegetation using airborne laser scanning.

Oettel, J., K. Lapin, G. Kindermann, H. Steiner, K.-M. Schweinzer, G. Frank, and F. Essl. 2020. Patterns and drivers of deadwood volume and composition in different forest types of the Austrian natural forest reserves. Forest Ecology and Management **463**:118016.

Ohmann, J. L., and M. J. Gregory. 2002. Predictive mapping of forest composition and structure with direct gradient analysis and nearest-neighbor imputation in coastal Oregon, USA. Canadian Journal of Forest Research **32**:725-741.

Packalén, P., and M. Maltamo. 2007. The k-MSN method for the prediction of species-specific stand attributes using airborne laser scanning and aerial photographs. Remote Sensing of Environment **109**:328-341.

Pal, D., V. Bundele, B. Banerjee, and Y. Jeppu. 2022. SPN: Stable Prototypical Network for Few-Shot Learning-Based Hyperspectral Image Classification. IEEE Geoscience and Remote Sensing Letters **19**:1-5.

Pedlar, J. H., J. L. Pearce, L. A. Venier, and D. W. McKenney. 2002. Coarse woody debris in relation to disturbance and forest type in boreal Canada. Forest Ecology and Management **158**:189-194.

Pesonen, A., A. Kangas, M. Maltamo, and P. Packalén. 2010. Effects of auxiliary data source and inventory unit size on the efficiency of sample-based coarse woody debris inventory. Forest Ecology and Management **259**:1890-1899.

Pesonen, A., M. Maltamo, K. Eerikäinen, and P. Packalèn. 2008. Airborne laser scanning-based prediction of coarse woody debris volumes in a conservation area. Forest Ecology and Management **255**:3288-3296.

Pyörälä, J., N. Saarinen, V. Kankare, N. C. Coops, X. Liang, Y. Wang, M. Holopainen, J. Hyyppä, and M. Vastaranta. 2019. Variability of wood properties using airborne and terrestrial laser scanning. Remote Sensing of Environment **235**:111474.

Raber, G. T., J. R. Jensen, S. R. Schill, and K. Schuckman. 2002. Creation of digital terrain models using an adaptive lidar vegetation point removal process. Photogrammetric engineering and remote sensing **68**:1307-1314.

Ranius, T., O. Kindvall, N. Kruys, and B. G. Jonsson. 2003. Modelling dead wood in Norway spruce stands subject to different management regimes. Forest Ecology and Management **182**:13-29.

Riffell, S., J. Verschuyl, D. Miller, and T. B. Wigley. 2011. Biofuel harvests, coarse woody debris, and biodiversity – A meta-analysis. Forest Ecology and Management **261**:878-887.

Roesch, F. A., and G. G. Moisen. 2005. 2 The Forest Inventory and Analysis Sampling Frame. The Enhanced Forest Inventory and Analysis Program--national Sampling Design and Estimation Procedures:11.

Safonova, A., S. Tabik, D. Alcaraz-Segura, A. Rubtsov, Y. Maglinets, and F. Herrera. 2019. Detection of Fir Trees (Abies sibirica) Damaged by the Bark Beetle in Unmanned Aerial Vehicle Images with Deep Learning. Remote Sensing **11**:643.

Scott, C. T. 1998. Sampling methods for estimating change in forest resources. Ecological Applications **8**:228-233.

Seielstad, C. A., and L. P. Queen. 2003. Using Airborne Laser Altimetry to Determine Fuel Models for Estimating Fire Behavior. Journal of Forestry **101**:10-15.

Shang, C., P. Treitz, J. Caspersen, and T. Jones. 2017. Estimating Stem Diameter Distributions in a Management Context for a Tolerant Hardwood Forest Using ALS Height and Intensity Data. Canadian Journal of Remote Sensing **43**:79-94.

Shokirov, S., M. Schaefer, S. R. Levick, T. Jucker, J. Borevitz, I. Abdurahmanov, and K. Youngentob. 2021. Multi-platform LiDAR approach for detecting coarse woody debris in a landscape with varied ground cover. International Journal of Remote Sensing **42**:9324-9350.

Shorten, C., and T. M. Khoshgoftaar. 2019. A survey on image data augmentation for deep learning. Journal of big data **6**:1-48.

Siitonen, J., P. Martikainen, P. Punttila, and J. Rauh. 2000. Coarse woody debris and stand characteristics in mature managed and old-growth boreal mesic forests in southern Finland. Forest Ecology and Management **128**:211-225.

Sullivan, A. A., R. J. McGaughey, H.-E. Andersen, and P. Schiess. 2009. Object-Oriented Classification of Forest Structure from Light Detection and Ranging Data for Stand Mapping. Western Journal of Applied Forestry **24**:198-204.

Sullivan, T. P., D. S. Sullivan, P. M. F. Lindgren, and D. B. Ransome. 2012. If we build habitat, will they come? Woody debris structures and conservation of forest mammals. Pages 1456-1468 Journal of Mammalogy.

Sun, X., B. Wang, Z. Wang, H. Li, H. Li, and K. Fu. 2021. Research Progress on Few-Shot Learning for Remote Sensing Image Interpretation. IEEE Journal of Selected Topics in Applied Earth Observations and Remote Sensing **14**:2387-2402.

Thiel, C., M. M. Mueller, L. Epple, C. Thau, S. Hese, M. Voltersen, and A. Henkel. 2020. UAS Imagery-Based Mapping of Coarse Wood Debris in a Natural Deciduous Forest in Central Germany (Hainich National Park). Remote Sensing **12**:3293.

Thomas, J. W. 1979. Wildlife habitats in managed forests: the Blue Mountains of Oregon and Washington. Wildlife Management Institute.

Van Dyk, D. A., and X.-L. Meng. 2001. The art of data augmentation. Journal of Computational and Graphical Statistics **10**:1-50.

Villon, S., C. Iovan, M. Mangeas, T. Claverie, D. Mouillot, S. Villéger, and L. Vigliola. 2021. Automatic underwater fish species classification with limited data using few-shot learning. Ecological Informatics **63**:101320.

Villon, S., C. Iovan, M. Mangeas, and L. Vigliola. 2022. Confronting Deep-Learning and Biodiversity Challenges for Automatic Video-Monitoring of Marine Ecosystems. Sensors **22**:497.

Waddell, K. L. 2002. Sampling coarse woody debris for multiple attributes in extensive resource inventories. Ecological Indicators **1**:139-153.

Waddell, K. L., and J. L. Ohmann. 2002. Regional Patterns of Dead Wood in Forested Habitats of Oregon and Washington. USDA Pacific Southwest Research Station.

Wang, Y., M. Lehtomäki, X. Liang, J. Pyörälä, A. Kukko, A. Jaakkola, J. Liu, Z. Feng, R. Chen, and J. Hyyppä. 2019. Is field-measured tree height as reliable as believed – A comparison study of tree height estimates from field measurement, airborne laser scanning and terrestrial laser scanning in a boreal forest. ISPRS Journal of Photogrammetry and Remote Sensing **147**:132-145.

Warren, W. G., and P. F. Olsen. 1964. A Line Intersect Technique for Assessing Logging Waste. Forest Science **10**:267-276.

Wei, Z., K. Jia, X. Jia, P. Liu, Y. Ma, T. Chen, and G. Feng. 2022. Mapping Large-Scale Plateau Forest in Sanjiangyuan Using High-Resolution Satellite Imagery and Few-Shot Learning. Remote Sensing **14**:388.

Westfall, J. A., A. J. Lister, C. T. Scott, and T. A. Weber. 2019. Double sampling for post-stratification in forest inventory. European Journal of Forest Research **138**:375-382.

White, J. C., M. A. Wulder, A. Varhola, M. Vastaranta, N. C. Coops, B. D. Cook, D. Pitt, and M. Woods. 2013. A best practices guide for generating forest inventory attributes from airborne laser scanning data using an area-based approach. The Forestry Chronicle **89**:722-723.

Windrim, L., M. Bryson, M. McLean, J. Randle, and C. Stone. 2019. Automated Mapping of Woody Debris over Harvested Forest Plantations Using UAVs, High-Resolution Imagery, and Machine Learning. Remote Sensing **11**:733.

Wing, B. M., M. W. Ritchie, K. Boston, W. B. Cohen, A. Gitelman, and M. J. Olsen. 2012. Prediction of understory vegetation cover with airborne lidar in an interior ponderosa pine forest. Remote Sensing of Environment **124**:730-741.

Woldendorp, G., R. J. Keenan, S. Barry, and R. D. Spencer. 2004. Analysis of sampling methods for coarse woody debris. Forest Ecology and Management **198**:133-148.

Woldendorp, G., R. Spencer, R. Keenan, and S. Barry. 2002. An analysis of sampling methods for coarse woody debris in Australian forest ecosystems. Bureau of Rural Sciences, Canberra.

Zald, H. S. J., J. L. Ohmann, H. M. Roberts, M. J. Gregory, E. B. Henderson, R. J. McGaughey, and J. Braaten. 2014. Influence of lidar, Landsat imagery, disturbance history, plot location accuracy, and plot size on accuracy of imputation maps of forest composition and structure. Remote Sensing of Environment **143**:26-38.

Zald, H. S. J., M. A. Wulder, J. C. White, T. Hilker, T. Hermosilla, G. W. Hobart, and N. C. Coops. 2016. Integrating Landsat pixel composites and change metrics with lidar plots to predictively map forest structure and aboveground biomass in Saskatchewan, Canada. Remote Sensing of Environment **176**:188-201.

Chapter 2: A Deep Learning Model for Large Coarse Woody Debris Prediction from Aerial LiDAR on the Malheur National Forest

1. Introduction

Down wood is an essential component of forest ecosystems and supports natural history requirements for a diverse array of wildlife species. Species diversity and abundance, especially of avian and small mammal species, are positively correlated with the quantity of down wood available on the landscape (Riffell et al., 2011; Sullivan et al., 2012). Johnson & O'Neil (2018) identified 96 wildlife species associated with down wood habitat in Oregon and Washington, many of which are species of concern as designated by federal and state agencies (Johnson & O'Neil, 2018). Coarse woody debris (CWD), also referred to as coarse woody material (CWM), is an umbrella term for larger pieces of down wood, with the exact cut-off specifications varying regionally and by institution. The USDA Forest Service Forest Inventory and Analysis (FIA) protocol define CWD as down wood greater than or equal to 30 inches in diameter and at least .0.5 feet in length (USDA Forest Service 2022). In practical studies of wildlife habitat, a larger cut off diameter of closer to 10 inches for CWD is common. These larger pieces are particular valuable to wildlife species (Rondeux et al., 2010). In broad terms, CWD provides cover, hunting grounds, travel corridors, microclimates, and substrate for invertebrates and fungi for forest vertebrates (Bunnell & Houde, 2010). An accurate understanding of CWD distribution help land managers ensure adequate coverage of habitat elements across the landscape.

However, CWD distribution is highly variable. Down wood distribution patterns in Oregon and Washington show significant regional variation and have been found to be non-normally distributed (Ohmann & Waddell, 2002; White et al., 2013). Additionally, CWD does not correlate consistently with other easily measurable site characteristics (Chojnacky & Heath, 2002).The dynamics driving distribution depends on several complex factors including successional stage, forest structure, management history, and community composition. (Harmon et al., 1986; Hofgaard, 1993). Accurate field measurements of down wood are particularly onerous to capture due to this heterogeneity across the landscape (Woldendorp et al., 2004). Given monetary and temporal constraints to increasing field efforts, managers look toward remote sensing in lieu of, or in conjunction with, traditional field inventories.

The USFS Pacific Northwest Region (PNW, Region 6) currently relies on a Gradient Nearest Neighbor (GNN) imputation model that integrates FIA field data with two-dimensional LANDSAT imagery in order to calculate down wood at broad scales across the landscape (Ohmann & Gregory, 2002). This mapping effort is central to the Decayed Wood Advisor (DecAID) platform: a management tool that catalogs down wood conditions for reference and current conditions and describes wildlife habitat on federally managed lands in the PNW. Although DecAID is a powerful management tool, it is

most robust at broader spatial scales and even then, the accuracy varies. Hence, there is a need for better estimates of CWD at smaller scales such as at the project or stand-level.

Active sensor technology like aerial laser scanning (ALS), also known as plane mounted LiDAR sensors, offer the potential to capture forest structure metrics on smaller scales with increased accuracy compared to methods that use satellite imagery alone (Zald et al., 2014). Unlike passive sensors that reflect energy from the sun, such as LANDSAT, active sensors generate their own energy and can provide information on the elevation profile through analyzing the return time intervals (Dubayah & Drake, 2000; Magnussen & Boudewyn, 1998). Previous studies have used ALS to quantify CWD through a variety of methodologies including indirect area based modeling approaches (Bater et al., 2007; Pesonen et al., 2008; Seielstad & Queen, 2003; van Aardt et al., 2011), analysis of LiDAR derived raster layers (Lindberg et al., 2013; Queiroz et al., 2020), comparison of changes in elevation height models over time (Nyström et al., 2014), and, more recently, direct measurement of the point cloud (Jarron et al., 2020, 2021; Joyce et al., 2019). Mücke et al. (2013) used discrete ALS data to create modified raster layers of the earth's surface and derived measures of surface roughness from which they manually extracted linear CWD features; identifying 77.8% of the CWD in the study area. Shokirov et al. (2021) also derived layers of surface characteristics from high-resolution multiplatform LiDAR but used an automated Random Forest (RF) Machine Learning (ML) method to identify pixels associated with CWD. Through this exercise they found surface roughness, a measure of the largest inter-cell difference of a focal cell and its 8 neighboring pixels, to be the most significant variable for CWD identification (Amatulli et al., 2018; Shokirov et al., 2021).

Object detection and image segmentation are branches of machine learning that extracts and analyzes pixels in meaningful groups (Hossain & Chen, 2019). Blanchard et al. (2011) used object based image analysis (OBIA) on ALS raster layers to identify 73% of pieces of large down wood (defined by small end diameter greater than or equal to 9.8 inches and a minimum length greater than or equal to 16.4 feet) in California but the required manual inputs for segmentation and analysis were time consuming and inefficient (Blanchard et al., 2011). Several studies have since attempted to further automate this deep learning process. Krisanski et al. (2021) found that automated segmentation and classification of the forest understory through Density-based spatial clustering of applications with noise (DBSCAN) unsupervised classification of merged terrestrial laser scanning (TLS) and ALS data sets achieved 54.98% accuracy in identifying coarse down wood with extremely high resolution input data (Krisanski et al., 2021). Windrim et al. (2019) automated volume estimates of CWD from high-resolution drone based LiDAR on a post-harvest pine plantation using automated detection and segmentation (Windrim et al., 2019).

In Deep Learning (DL), a specific subset of machine learning, a computer learns to recognize and identify objects through convolutional neural network (CNN). Mask Region Based CNN (Mask R-CNN) is a novel methodology in deep learning that detects and segments objects from an image with high accuracy and requires little input from the user beyond initial training samples (He et al., 2017). These new deep learning technique remove many of the previous manual inefficiencies in machine learning detection of CWD. Until this point, DL has not been applied to ALS based CWD quantification, particularly not at the project area or landscape level scale.

This research employs Mask R-CNN deep learning on ALS derived surface layers in order to detect and segment individual pieces of CWD and create estimates of percent cover of CWD across the project area. The advantage of this method is the ability to obtain wall-to-wall estimates at smaller scales needed for making management decisions at a stand-level. These estimates will be compared to DecAID, the current tool being used, and field data collected using FIA transect protocols for CWM. An analogous definition of CWD will be used in this methodology to facilitate comparisons between deep learning and the GNN imputation. CWD is therefore defined as pieces of down wood with a diameter greater than or equal to .85 feet and a length greater than or equal to 9 feet. We hypothesize that this method will improve the accuracy of CWD percent cover estimates when compared to GNN.

2. Materials and Methods

2.1. Study Area

This study was conducted on the Malheur National Forest in eastern Oregon. The Malheur National Forest is located within the Blue Mountains region of Oregon. The strawberry mountains, a subrange of the Blue Mountains, run east to west through the northern part of the study area. The study area is comprised of two non-contiguous locations, one near Upper Bear Lake (31,137 acres) and the other near Canyon Creek (68,069 acres, **Figure 1**). This area is dominated by dry upland forest where ponderosa pine (*Pinus ponderosa),* white fir (*Abies concolor*) and lodgepole pine (*Pinus contorta*) are most abundant. The majority of the study area is sparsely forested and canopy closure is rarely above 60% (Hummel et al., 2011). Elevation varies from approximately 4,000 to a maximum of 9,038 feet at the summit of Strawberry Peak. This area experiences short, dry summers and long, cold winters, with minimum winter temperatures falling between 18 and 19 degrees Fahrenheit and maximum summer temperature ranging between 64 and 76 degrees Fahrenheit. Monthly precipitation averages from 0.5 inches in the summer to almost 5 inches during the wettest, winter months (PRISM Climate Group, 2021).

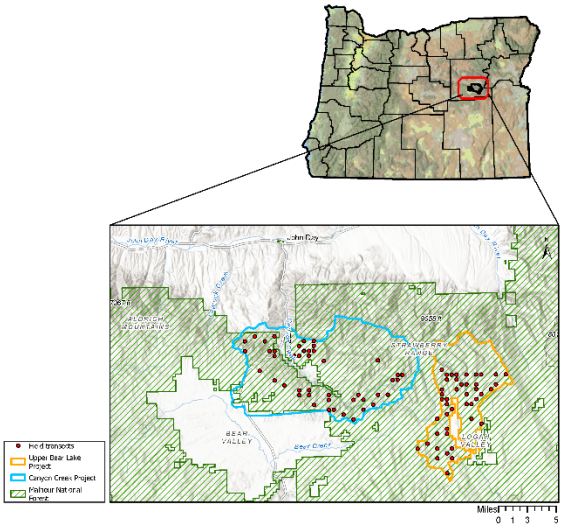

Figure 1. Map of project area with inset for the state of Oregon. The project areas are defined by the blue and orange polygons and the dots, the field plot locations.

2.2. Data Collection

A Cessna Grand Caravan plane was used to acquire ALS data across the study site between June 14 and July 9, 2017. The raw data was initially processed by Quantum Spatial, Inc (QSI) for the USFS in 2017 (**Table 1**). The processed files contained an average resolution of at least eight pulses per square meter throughout the study site. All files were projected in Oregon Lambert with a NAD83 (2011) horizontal datum and NAVD88 (Geoid 12B) vertical datum, with units in International feet (QSI, 2018). The data was accessed through the Oregon Department of Geology and Mineral Industries (DOGAMI) website on April 11, 2021.

Table 1. Specifications of ALS data

Program	**Oregon Lidar Consortium**
Project	John Day 3DEP 2017
Acquisition date	June 4, 2017- July 9 2017
Area (sq miles)	1,096.3
Horizontal datum	NAD 1983 (2011)
Vertical Datum	NAVD88 (GEOID 12B)
Projection	NAD 1983 (2011) Oregon Statewide
Resolution	3 feet / 1 meter
Sensory type	Leica ALS 50 Phase II
Collection height	1,500 meters ABL
Pulse density	Average of 11.80 pulses per square meter

One hundred field plots were installed across the study site and measured between July 2016 and October 2019. Care was taken to ensure all field data was collected within two years of ALS acquisition. Data was collected in adherence to FIA protocols for down wood (Burrell 2021). Two 24-foot transects were located at each plot location, one ran due east and the other due west from plot center. For each transect, CWD, defined as greater than three inches in diameter at the short end and greater than five inches in length was recorded. Diameter, length, and decay class were measured and recorded for every piece where the central longitudinal axis of the CWD intersected with the transect. A single log was tallied as two separate pieces if it is fractured to an extent that it could easily split into components if pulled apart (*Region 6 PNW LiDAR Field Plot Procedures*, 2019). Following FIA cut off thresholds for CWD, 106 pieces of CWD were tallied across 69 of the 100 field plots. The average CWD diameter was 14.1 inches, with the majority of pieces falling under 15 inches. The pieces ranged in length from 9 to 110 feet, with an average of 39.3 feet. Decay class was defined for five categories within the FIA protocol. The CWD was centered around a decay class of three, indicating that the majority of logs were moderately decayed; these logs are described as being hard, large pieces able to support their own weight, absent sapwood, which could be pulled apart by hand and the original color of the wood has begun to redden or change (**Figure 2**) (*Region 6 PNW LiDAR Field Plot Procedures*, 2019).

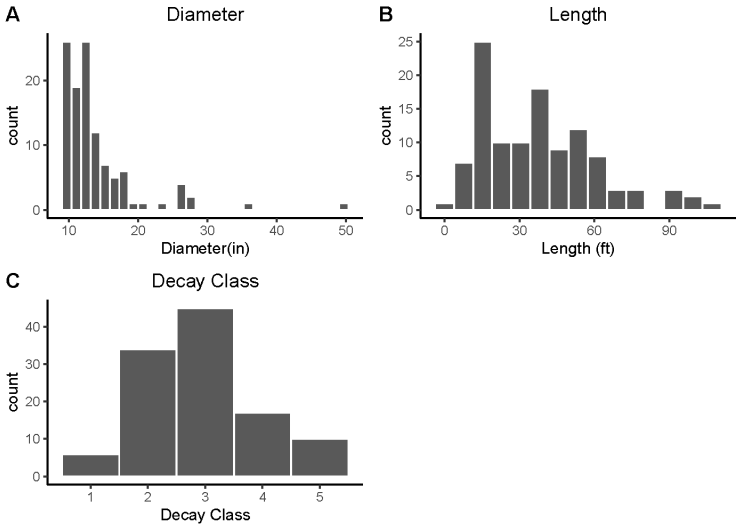

Figure 2. Frequency distributions for the coarse woody debris metrics: (A) diameter, (B) length, and (C) decay class.

2.3. Data Processing

The overall workflow of preprocessing, deep learning (training & detection), post-processing, and validation are shown in **Figure 3** and described below.

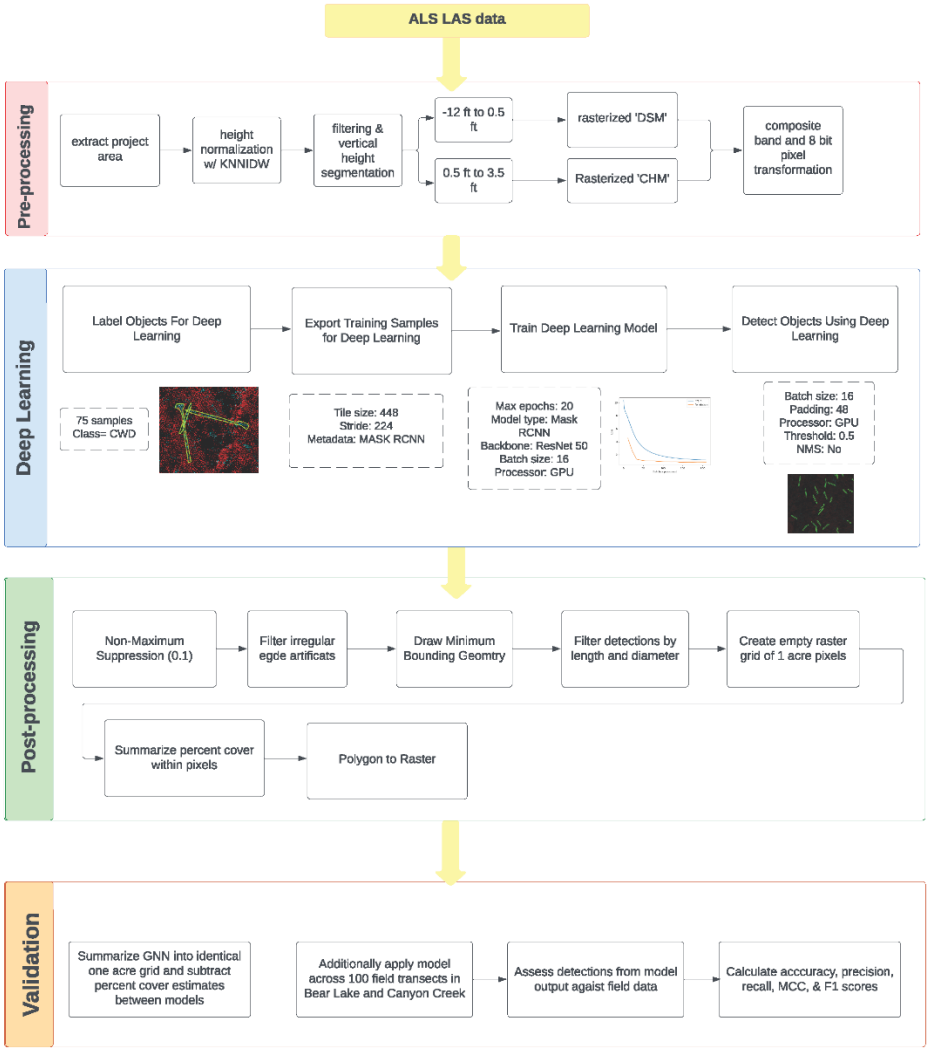

Figure 3. Work flow diagram of data preprocessing, deep learning, post processing, and validation.

2.3.1. Preprocessing

ALS point clouds were processed in R and R Studio (2022.02.1), using the LiDR package (version 4.0.0) (Roussel et al., 2020). The LAScatalog processing engine functionality of the package was employed to cut down processing time and issues with device storage in consideration of large point cloud files. LAS files were clipped to the project area boundaries using a buffer of 50 feet, approximately one half the length of a large tree. It has been shown that inaccurate ground segmentation can obscure CWD pieces near the forest floor (Brubaker et al., 2013). Ground segmentation initially processed by QSI was visually assessed throughout the point cloud and found to be more accurate than other common ground classification algorithms (e.g. cloth simulation filter (W. Zhang et al., 2016) and progressive

morphological filter (K. Zhang et al., 2003)). The point cloud height values were normalized using a spatial interpolation approach based on a k-nearest neighbor (KNN) with an inverse-distance weighting.

To isolate the point cloud data which represents the vertical structure of the forest where CWD would be present, a threshold value was used to segment the point cloud. The threshold value was selected based upon the field measured CWD distributions found from the transect data. While the largest diameter of CWD in the study area was 50 inches, the diameter distribution is highly right-skewed. Due to the skewness of the distribution and the understanding that large downed logs will depress the ground where they fall, 42 inches was selected as an appropriate threshold value for segmenting the point cloud. This value was also selected to exclude noise in the point cloud data from tall understory vegetation.

Previous work shows that multi-return pulses near the forest floor are more likely associated with deciduous shrubs and leaves as compared to down wood (Béland et al., 2014; Raber et al., n.d.). Following this rationale all multi-return pulses were also excluded from the point cloud data. The remaining points were then rasterized into two surfaces, from one half to three and a half feet in elevation and points below half a foot in elevation. Both rasterized surfaces were created using a pixel resolution of half a foot and exported as raster files for the entire study area.

2.3.2. Deep Learning

Deep learning framework was applied in ArcGIS pro (2.9.3) using a composite raster layer with two bands created from the surface layers created in the pre-processing stage. The composite raster layer was transformed from 32 bit float pixels into 8 bit unsigned pixels with the values scaled.

The first step of the deep learning process was to identify a training location from which training data could be obtained. Care was taken to select a representative training location outside of the study area with similar elevation and a representative pattern of CWD. The training location was then compared visually to the study area using the National Agriculture Imagery Program (NAIP) imagery to ensure the species composition and spatial distribution of trees were similar. An ALS quad of one square mile was selected adjacent to the Upper Bear Lake study area as the training location.

The second step of the deep learning process was to create a training data set of CWD from the training location. A feature class of training samples for CWD was created by manually delineating seventy-five CWD objects. The training location was visually assessed for visible pieces of CWD using a combination of validation techniques. Pieces of CWD were selected only if they were clearly visible in the rasterized layers and at least partially suggested in the underlying imagery either from Esri or NAIP imagery. Other parameters for selection included a clear beginning and terminus, with particular preferences given to pieces with characteristic taper shapes or root bole shapes.

Once CWD was identified, polygons were digitized around the pieces to encompass the entirety of the log including a small buffer of ground surrounding the piece. The buffer was included as the area

surrounding the down log is likely to have fewer points that fall directly underneath the curvature of the log, creating a unique pattern within the point cloud. Training samples were located across the entire training location in order to capture as much geographic variability as possible.

Next, using an image analyst tool called 'Export Training Data for Deep Learning", the training data was used to generate image chips containing the class sample from the source image and a folder of associated Mask regions with convolutional neural network**s** (R-CNN) metadata. Image chips were exported in a TIFF format, with CWD as the class field, no buffers, 448x448 tile size, an map reference system, and a Mask R-CNN metadata format (Everingham et al., 2015; He et al., 2017). During model training, the image chips are repetitively run through the neural network until the model learns to identify the important characteristics of CWD. 20 epochs were run on a resnet50 backbone with a batch size of 16.

Finally the trained model was then used to detect individual pieces of CWD within the study area. The model was applied across the entire study area including each of the 100 field plot transects located within the study area. Each detection of CWD was returned as a polygon with as associated confidence attribute.

2.3.3. Post Processing

Post processing of detected CWD was undertaken to increase accuracy and summarize individualize detections as a measure of percent cover. In order to remove the majority overlapping returns, all detections were run through non maximum suppression with a maximum overlap ratio of 0.1. Detections were clipped to the project boundary to avoid irregular detections along raster edges. A minimum geometry bounding box was drawn around each detection in order to calculate the length and width of each polygon. Detections were then further filtered based on several size classifications. GNN estimates percent cover of wood greater than or equal to 9.84252 inches in diameter and greater than or equal to nine feet in length: a larger size threshold distinction for CWD than used by FIA. To facilitate comparison between methodologies, the GNN thresholds were used and all detections below that specified length or diameter were removed. To further remove any potential irregularly large detections, any detection over the length of the height of the tallest tree in the project area was also removed. Finally, any remaining, overlapping polygons were dissolved into singular polygons.

An empty fishnet grid with square one acre pixels was overlaid across the entire project area. Percent cover was then calculated as total area of detected CWD polygons within each on acre pixel. This percent cover shapefile was then rasterized to visualize percent cover across the entire study area.

2.3.3. Model Assessment and Validation

The detections from the deep learning (DL) model were compared to the field data from the one hundred field transects and estimates obtained from the GNN imputation model (*Gradient Nearest Neighbor (GNN) Raster Dataset (Version 2020.01)*). The GNN imputation model delivers percent cover

estimates across 30 x 30 m pixels. In order to compare the GNN estimates to the DL model, GNN estimates were re-calculated as weighted averages across a spatially identical one acre fishnet. Any "non-forested" areas excluded in the GNN data were assumed to have zero percent cover. The differences between the DL model and the GNN estimates were mapped across the study site to assess any geographic patterns.

To assess the model, accuracy, precision, and recall values were calculated as follows:

$$Accuracy = \frac{True\ Positive + True\ Negative}{Overall\ Total}$$

$$Precision = \frac{True\ Positive}{True\ Positive + False\ Positive}$$

$$Recall = \frac{True\ Positive}{True\ Positive + False\ Negative}$$

Where all values are defined by the confusion matrix (**Table 2**). Accuracy is the ratio of correctly predicted observation to the number of total observations. Precision is a measure of how well a model preforms at positive classification. High precision rates imply the model has a low false positive rate. The recall score reflects the proportion of actual positives that were correctly identified. A model with no false negatives will have a recall of 1.0 (Padilla et al., 2020).

Table 2. Confusion matrix.

		Predicted (Machine Learning Model)	
		Negative	*Positive*
Actual (Field Transects)	*Negative*	True Negative (TN)	False Negative (FN)
	Positive	False Positive (FP)	True Positive (TP)

A F1 score is a validation metric of binary classification that is the harmonic mean of precision, which measures the extent of errors caused by false positives (FP) and recall, which measures the extent

of errors caused by false negatives (FN). F1 scores closer to 1 represent the most accurate models. F1 was calculated as:

$$F1 = \frac{2(Precision * Recall)}{Precision + Recall}$$

In addition, the Mathew's Correlation Coefficient (MCC) was calculated. In a two by two matrix, MCC is identical to the phi coefficient (φ) which measures the association between two binary variables. In a machine learning setting, MCC is a measure of the quality of binary classifications. The closer MCC or κ are to a value of one, the better the model is at classifying the data correctly; values closer to negative one predict every value (Chicco and Jurman 2020). MCC was calculated as:

$$MCC = \frac{TP * TN - FP * FN}{\sqrt{(TP + FP)(TN + FN)(TN + FP)(TP + FN)}}$$

3. Results

The deep learning model detected 27,096 CWD class objects across the Upper Bear lake project area, with percent cover ranging from 0 % to 10.28 % across the one acre pixels (**Figure 4**). The field data collected on the transects indicate that the distribution of the percent cover of CWD is skewed, with many areas having no CWD. Compared to the field data, the DL model better predicts the range of percent cover better than GNN, at least for the extreme values. This can be seen by comparing the maximum values to the field data maximum (over 12%), approximately 10% and less than 6% respectively. These areas of higher percent cover predicted by the DL model are supported by several transect areas which reflect areas of higher percent cover not otherwise captured in GNN. These areas of higher percent cover are also visually apparent across the landscape. In addition, the median value from the DL model more accurately reflects the skewness found from the field data. The DL model estimated overall lower percent cover across the project area and significantly more acres with zero percent cover than the GNN model. The same detections are visualized across NAIP imagery and across the rasterized surface layers in **Figure 5**.

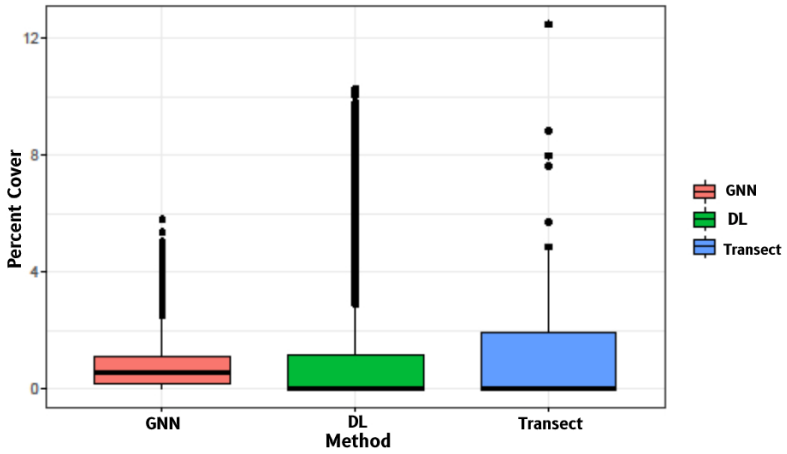

Figure 4. Distribution of percent cover estimates from the DL model, the GNN model, and field transects.

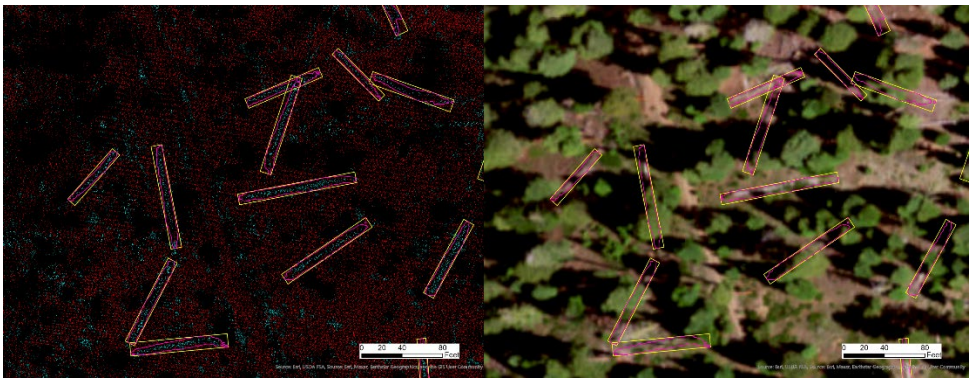

Figure 5. Detections from DL model shown over NAIP satellite imagery (right) and rasterized ALS layers (left)

The spatial arrangement of the difference in percent cover estimates between the DL model and the GNN estimates can be found in **Figure 6**. The majority (66%) of the one acre pixels indicate that the difference between the DL model and the GNN estimates were within plus or minus 1%. A higher degree of agreement was found in areas with overall lower CWD, whereas estimates differed more significantly in areas with higher CWD amounts. Visual inspection of incongruous areas revealed that the DL model performed poorer in areas of ecological transitions (**Figure 7**). Detections were generally lower in open areas with large quantities of down wood arranged in complex distribution patterns (i.e. areas following disturbance like logging).

In addition, overlapping CWD also presented a detection problem (**Figure 8**). The field data records two pieces of CWD on the transect. The first is 20 inches in diameter, 44 feet in length, and decay class 4 (piece A) and the second is 26 inches in diameter, 60 feet in length, and decay class 3 (piece B). Visual inspection of the photograph reveals that the two pieces overlap one another in a cruciform alignment with the shorter more decayed log (A) on bottom and the larger log (B) on top running northwest to southeast. The deep learning model detected one piece of CWD in this area that matches

piece A. Although one might expect the larger, the less decayed piece was more easily detected, the fact that B is lying on top of A means less of the log is in contact with the ground. The DL model detects CWD objects through the elevation change and relationship between the log and the ground. The detected CWD object from the DL model measures 61 feet in length, less than the recorded field length for the same log of 44 feet. One possible explanation for this discrepancy in length is the nuance that CWD pieces with significant splits or cracks are considered two objects for the sake of field data collection. Piece A is fractured in the middle where B fell on top of it and measuring to the point of intersection from the DL model gives a length of 34 feet, a length much closer to the field data.

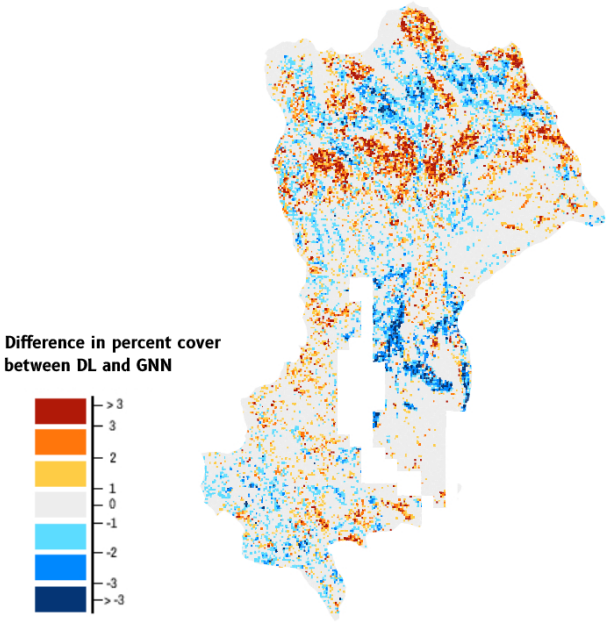

Figure 6. Spatial distribution of the difference in percent cover estimates over one acre pixels as predicted by DL and GNN. Difference calculated as DL percent cover estimate – GNN percent cover estimate. Grey pixels show where the models predicted within +- 1 % cover of each other. Warmer colors highlight areas where the DL model predicted higher percent cover than GNN.

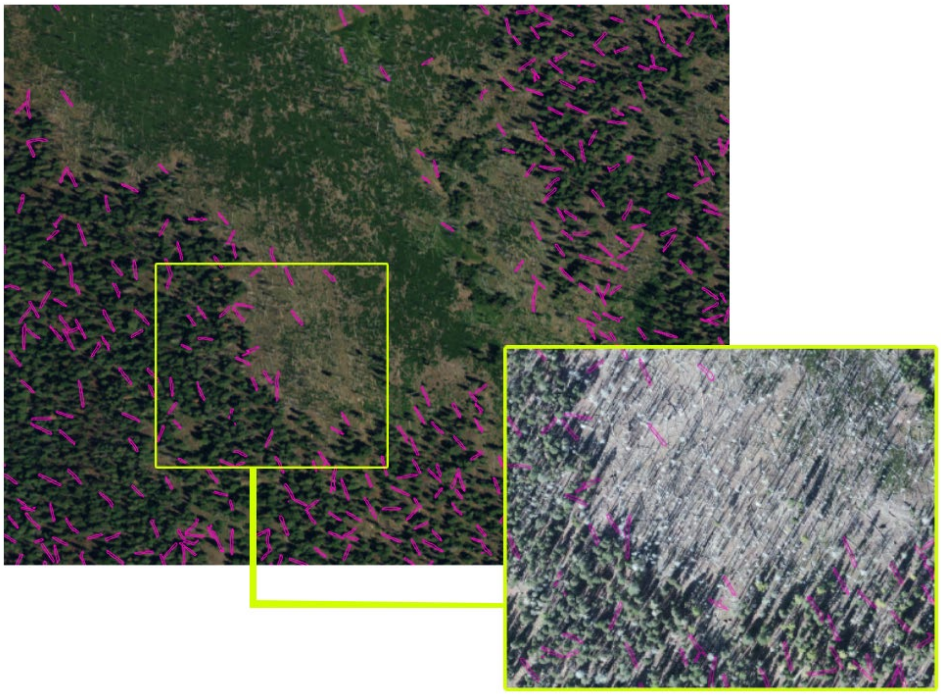

Figure 7. Patterns of machine learning detections (pink) follow stand borders. Fewer detections in the area with more complex pattern of CWD.

Figure 8. (Left) Photo of field transect looking N with yellow dotted line representing transect. (Right) Aerial imagery of same field transect. Green circle is subplot diameter. Blue dot is transect center. Pink is detected object from DL model. A and B highlight the same two logs visible in each frame with field transect information in bottom right.

Accuracy was found to be 0.5913, precision 0.750, and recall 0.0612 (**Table 3**). The DL model was accurate just under 60 percent of the time. The precision value indicates that 75 percent of the predicted CWD logs were actually CWD logs, however, the low recall value (0.0612) indicates that for those CWD logs found on a transect, the DL model did a poor job of predicting them. Both the MCC and

F1 score are close to a value of zero, indicating that there is a weak association between the predicted and actual CWD logs.

Table 3. Validation metrics for machine learning model.

Validation Metric	Result
Accuracy	0.5913
Precision	0.750
Recall	0.0612
MCC	0.1243
F1	0.1132

4. Discussion

While the high precision combined with low recall score suggests that the DL model is conservative at detecting CWD objects; there is a high level of accuracy on positive detections. The overall low sample size of CWD logs from the transect data make the precision value and the recall score unreliable on their own. The F1 score is known to be a more appropriate measure for unbalanced data sets. Although the F1 score was lower than anticipated, there is still evidence to suggest the DL model provides useful information for managers and that may be providing more accurate information than the current model in use (GNN). While the range of percent cover from all three methodologies was similar, the mean for both the DL and field transects were lower (Figure 3). GNN has a smaller range but a higher mean. The DL model includes a wider range of values that better captures the true variability seen across the landscape, as is reflected in the field transects. These findings corroborate complaints from managers that GNN tends to over-estimate the amount of CWD on the landscape.

While each of the transect locations was known, the lack of spatial information for each piece of CWD, such as position across the transect or axes in space, made it difficult to assess the DL predictions with field measurements to a high degrees of accuracy; this was particularly true in instances where logs overlapped. Certain nuances in the field protocols further complicated this validation. For example, logs with central break points are tallied as two separate pieces in the field but that small scale information is likely lost from LiDAR point cloud data and the log would register as a single entity in this methodology. A handful of transects were photographed and these photographs, where they exist, can aid in matching and validation.

There was an inadequate number of CWD pieces represented in this field data from which to draw training samples. The resulting need to rely on manual analysis of satellite imagery to identify CWD for training samples hindered inclusion of the full range of diversity of CWD physical properties, arrangement, and distribution. Strict adherence to required reasonable selection criteria for inclusion

meant that only the larger and most visually obvious (i.e. often less decayed) pieces of CWD were included. These criteria also resulted in uneven sampling across stand types on either extreme end of the spectrum of canopy cover. It is more difficult to visually identify CWD under dense forest cover where there is limited visibility in aerial imagery. Individual lone pieces were easier to accurately delineate than CWD pieces that overlapped. In open areas with large quantities of down wood or post-disturbance/post-management areas, there was an overabundance of noise that made it difficult to accurately identify where one piece of wood ended and a different began. As such, a skewed majority of delineated training samples were found in areas with medium to sparse canopy cover or areas with sparser cover.

The high variability of CWD across the landscape makes traditional field sampling efforts inadequate, leading to inaccurate estimates. The field transects captured a low number of CWD pieces, leading to a skewed data set inflated by a large number of zeros. This level of variation and the limitation of FIA data (i.e. approximately one plot per 1800 acres in this region of the USDA Forest Service) may lead to higher estimates of CWD. The distribution of CWD percent cover across the study area indicates a higher median value than either the DL or the transect data.

The pixels with the largest discrepancy between GNN and DL percent cover estimates are explored visually in **Figure 9.** The GNN model estimated below 1% cover for this acre while the DL model estimated 10.28% cover. Several down logs are visible in the aerial imagery from June 2017 and although exact measurements are difficult to ascertain, percent cover is almost certainly above 1% (the GNN estimate for this area). This highlights a weaknesses in the GNN imputation model. The number of FIA plots in the project area is limited (approximately one per 1800 acres of which ten percent is measured annually). There is also a time lag of processing between when FIA data is collected and processed till it becomes available for incorporation into the GNN model.

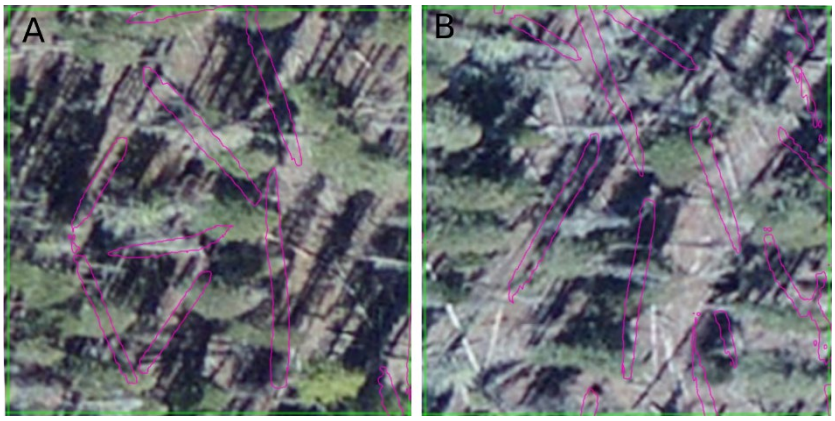

Figure 9. Two acres with large difference in percent cover estimates between the DL model and the GNN estimates. The GNN model predicted below 2% percent cover for both these acres (A: 1.179%, B: 0.629%), while the DL model predicted a much higher percent cover for both pixels (A: 9.488%, B: 10.050%). In the base map of ArcGIS World Imagery from June 2017, several down logs are visible in each image. A visual assessment of percent cover based on the visible logs suggests the GNN estimate is likely too low and that the DL estimates may be more accurate in these cases.

Size and decay class are both known to impact discovery rates of CWD (Jarron et al., 2021; Joyce et al., 2019). Every log correctly identified from the transect data (true positives) by the DL model had a diameter greater than or equal to 23 inches, a length of greater than or equal to 60 feet, and a decay class of less than 3 (decay class 1, 2, or 3). Decay class was not considered explicitly in the model and size was considered at an arbitrary threshold in order to compare outcomes to GNN estimates. When assessing only the CWD logs for decay class greater than 3 and above the thresholds used in GNN, pieces greater than or equal to 9.82 inches in diameter and greater than or equal to 9 feet in length, the F1 validation score increases to 0.75. Although the model performance improves for this larger size threshold, the sample size becomes too small to draw meaningful conclusions.

Managers interested in a specific wildlife species can filter detections to different thresholds in order to examine species specific use of different size pieces of CWD. For example, in the Blue Mountains, pine martens den on logs with a mean length of 79 feet and rest on logs with a mean length of 66 feet (Bull & Heater, 2000). Pileated woodpeckers most commonly foraged on logs larger than 49 feet in length (Bull et al., 1990). In addition to estimates of percent cover, this DL methodology provides information on physical arrangement and distribution of individual pieces of CWD across the landscape. This adds a valuable perspective in terms of wildlife habitat management as simple measurements of percent cover or volume over a set area are unable to capture the true dynamics of cover connectivity or travel corridors. The arrangement of CWD pieces on the ground also offers interesting insights as to the disturbance history of a site. For example, an area with abundant large CWD in the same direction could indicate a wind throw event.

More detailed and precise spatial information on field distribution of CWD for use in training and validation would likely result in higher model accuracy. However, given the variability in spatial patterns, it is unlikely to ever truly capture the full diversity of CWD dynamics. Additionally, the increased input of time and money required for more thorough field mapping to better attempt to capture these complex dynamics may not be worth the resulting increase in model accuracy when the application of the model is viewed in context of use. Although accuracy and completeness of detection varies across the project area, this tool will enable managers to focus resources more efficiently and effectively. Portions of project areas may be excluded from field efforts due to percent cover being measured over certain thresholds of interest. This also allows valuable monetary and time field resources to be directed towards areas of greater uncertainty, thereby increasing the efficacy of management.

A DL model may provide information that could be used in the sampling design process as a tool to increase efficiencies in field data collection. While validation results suggest the DL model is conservative, especially in open areas with high quantities of CWD, this information can still be used to identify areas above or below the management threshold for certain species. DECAID lists the 50% tolerance level for down wood percent cover for black bears in eastside mixed conifer forest as 2.6% cover of down wood >= 4 inches in diameter (Marcot et al., 2002). A manager interested in increasing down wood black bear habitat only needs to focus on areas below that threshold. All models balance a tradeoff between recall and precision. In the context of species conservation, particularly of sensitive species, it is more appropriate and safer to be under-estimating habitat quality than over-estimating.

5. Conclusions

Given the challenges in training and validation data, this study was unable to quantify the specific percent cover measurements of a wide range of CWD across the landscape as the initial research question intended. However, further exploration of the model output suggests a high degree of successful CWD detection, especially for larger pieces. This lends credence to the models ability to identify CWD in specific cases and still provide useful management information. Further exploration with higher density LiDAR dataset would likely increase the gains in using a DL model

REFERENCES

Amatulli, G., Domisch, S., Tuanmu, M. N., Parmentier, B., Ranipeta, A., Malczyk, J., & Jetz, W. (2018). A suite of global, cross-scale topographic variables for environmental and biodiversity modeling. Scientific Data 2018 **5**:1, 5(1), 1–15. https://doi.org/10.1038/sdata.2018.40

Bater, C., Coops, N. C., Gergel, S., & Goodwin, N. (2007). Towards the estimation of tree structural class in northwest coastal forests using lidar remote sensing. ISPRS Workshop on Laser Scanning, January, **38–4**3. http://www.isprs.org/proceedings/XXXVI/3-W52/final_papers/Bater_2007.pdf

Béland, M., Baldocchi, D. D., Widlowski, J. L., Fournier, R. A., & Verstraete, M. M. (2014). On seeing the wood from the leaves and the role of voxel size in determining leaf area distribution of forests with terrestrial LiDAR. Agricultural and Forest Meteorology, **184**, 82–97. https://doi.org/10.1016/J.AGRFORMET.2013.09.005

Blanchard, S. D., Jakubowski, M. K., & Kelly, M. (2011). Object-based image analysis of downed logs in disturbed forested landscapes using lidar. Remote Sensing, **3**(11), 2420–2439. https://doi.org/10.3390/rs3112420

Brubaker, K. M., Myers, W. L., Drohan, P. J., Miller, D. A., & Boyer, E. W. (2013). The Use of LiDAR Terrain Data in Characterizing Surface Roughness and Microtopography. Applied and Environmental Soil Science, 2013, **13**. https://doi.org/10.1155/2013/891534

Bull, E. L., & Heater, T. W. (2000). Resting and denning sites of American martens in northeastern Oregon. Northwest Science., **74**(3), 179–185.

Bull, E. L., Holthausen, R. S., & Henjum, M. G. (1990). Techniques for monitoring pileated woodpeckers. U.S. Department of Agriculture, Forest Service, Pacific Northwest Research Station. https://doi.org/10.2737/pnw-gtr-269

Bunnell, F. L., & Houde, I. (2010). Down wood and biodiversity - Implications to forest practices. Environmental Reviews, 18(1), 397–421. https://doi.org/10.1139/A10-019

Chicco, D., Warrens, M. J., & Jurman, G. (2021). The Matthews Correlation Coefficient (MCC) is More Informative Than Cohen's Kappa and Brier Score in Binary Classification Assessment. IEEE Access, **9**, 78368–78381. https://doi.org/10.1109/ACCESS.2021.3084050

Chojnacky, D. C., & Heath, L. S. (2002). Estimating down deadwood from FIA forest inventory variables in Maine. Environmental Pollution, **116**(SUPPL. 1). https://doi.org/10.1016/S0269-7491(01)00243-3

Dubayah, R. O., & Drake, J. B. (2000). Lidar remote sensing for forestry. Journal of Forestry, **98**(6), 44–46.

Everingham, M., Ali Eslami, S. M., Van Gool, L., I Williams, C. K., Winn, J., Zisserman, A., Everingham, M., A Eslami, S. M., Winn, J., Van Gool Leuven, L. K., Van Gool ETH, B. L., K I Williams, S. C., & Zisserman, A. (2015). The PASCAL Visual Object Classes Challenge: A Retrospective. Int J Comput Vis, **111**, 98–136. https://doi.org/10.1007/s11263-014-0733-5

Gradient Nearest Neighbor (GNN) raster dataset (version 2020.01). Modeled forest vegetation data using direct gradient analysis and nearest neighbor imputation. (2020). Landscape Ecology Modeling, Mapping, and Analysis (LEMMA) Team.

Harmon, M. E., Franklin, J. F., Swanson, F. J., Sollins, P., Gregory, S. V., Lattin, J. D., Anderson, N. H., Cline, S. P., Aumen, N. G., Sedell, J. R., Lienkaemper, G. W., Cromack, K., & Cummins, K. W. (1986). Ecology of Coarse Woody Debris in Temperate Ecosystems. Advances in Ecological Research, **15**(C), 133–302. https://doi.org/10.1016/S0065-2504(08)60121-X

He, K., Gkioxari, G., Dollár, P., & Girshick, R. (2017). Mask R-CNN.

Hofgaard, A. (1993). 50 years of change in a Swedish boreal old-growth Picea abies forest. Journal of Vegetation Science, **4**(6), 773–782. https://doi.org/10.2307/3235614

Hossain, M. D., & Chen, D. (2019). ISPRS Journal of Photogrammetry and Remote Sensing Segmentation for Object-Based Image Analysis (OBIA): A review of algorithms and challenges from remote sensing perspective. https://doi.org/10.1016/j.isprsjprs.2019.02.009

Hummel, S., Hudak, A. T., Uebler, E. H., Falkowski, M. J., & Megown, K. A. (2011). A comparison of accuracy and cost of LiDAR versus stand exam data for landscape management on the Malheur National Forest. Journal of Forestry, **109**(5), 267–273. https://doi.org/10.1093/jof/109.5.267

Jarron, L. R., Coops, N. C., MacKenzie, W. H., & Dykstra, P. (2021). Detection and Quantification of Coarse Woody Debris in Natural Forest Stands Using Airborne LiDAR. Forest Science, July, 1–14. https://doi.org/10.1093/forsci/fxab023

Jarron, L. R., Coops, N. C., MacKenzie, W. H., Tompalski, P., & Dykstra, P. (2020). Detection of sub-canopy forest structure using airborne LiDAR. Remote Sensing of Environment, **244**, 111770. https://doi.org/https://doi.org/10.1016/j.rse.2020.111770

Johnson, D. H., & O'Neil, T. (2018). Wildlife Habitat Relationships in Oregon and Washington.

Joyce, M. J., Erb, J. D., Sampson, B. A., & Moen, R. A. (2019). Detection of coarse woody debris using airborne light detection and ranging (LiDAR). Forest Ecology and Management, **433**, 678–689. https://doi.org/10.1016/J.FORECO.2018.11.049

Krisanski, S., Sadegh Taskhiri, M., Gonzalez Aracil, S., Herries, D., & Turner, P. (2021). Remote sensing Sensor Agnostic Semantic Segmentation of Structurally Diverse and Complex Forest Point Clouds Using Deep Learning. https://doi.org/10.3390/rs13081413

Lindberg, E., Hollaus, M., Mücke, W., Fransson, J. E. S., & Pfeifer, N. (2013). Detection of lying tree stems from airborne laser scanning data using a line template matching algorithm. ISPRS Annals of the Photogrammetry, Remote Sensing and Spatial Information Sciences, **2**(5W2), 169–174. https://doi.org/10.5194/isprsannals-II-5-W2-169-2013

Magnussen, S., & Boudewyn, P. (1998). Derivations of stand heights from airborne laser scanner data with canopy-based quantile estimators. Canadian Journal of Forest Research, **28**(7), 1016–1031.

Marcot, B. G., Mellen, K., Livingston, S. A., & Ogden, C. (2002). The DecAID advisory model: wildlife component. Laudenslayer, WF, Jr.; Valentine, B.; Weatherspoon, CP, 561–590.

Nyström, M., Holmgren, J., Fransson, J. E. S., & Olsson, H. (2014). Detection of windthrown trees using airborne laser scanning. International Journal of Applied Earth Observation and Geoinformation, **30**, 21–29. https://doi.org/10.1016/j.jag.2014.01.012

Ohmann, J. L., & Gregory, M. J. (2002). Predictive mapping of forest composition and structure with direct gradient and nearest-neighbor imputation in coastal Oregon, U.S.A. Canadian Journal of Forest Research, **32**(4), 725–741. https://doi.org/10.1139/x02-011

Ohmann, J. L., & Waddell, K. L. (2002). Regional Patterns of Dead Wood in Forested Habitats of Oregon and Washington. USDA Forest Service Gen. Tech. Rep, 97331, 535–560.

Padilla, R., Netto, S. L., & Da Silva, E. A. B. (2020). A Survey on Performance Metrics for Object-Detection Algorithms; A Survey on Performance Metrics for Object-Detection Algorithms. 2020 International Conference on Systems, Signals and Image Processing (IWSSIP).

Pesonen, A., Maltamo, M., Eerikäinen, K., & Packalèn, P. (2008). Airborne laser scanning-based prediction of coarse woody debris volumes in a conservation area. Forest Ecology and Management, **255**(8–9), 3288–3296. https://doi.org/10.1016/j.foreco.2008.02.017

PRISM Climate Group, Oregon State University, https://prism.oregonstate.edu, data created 4

Feb 2014, accessed 16 Dec 2020. (n.d.).

QSI. (2018). 2017 OLC John Day Data Report.

Queiroz, G. L., McDermid, G. J., Linke, J., Hopkinson, C., & Kariyeva, J. (2020). Estimating coarse woody debris volume using image analysis and multispectral LiDAR. Forests, 11(2). https://doi.org/10.3390/f11020141

Raber, G., Jensen, J., S. S.-… engineering and remote, & 2002.Creation of digital terrain models using an adaptive lidar vegetation point removal process. Asprs.Org. Retrieved March 14, 2022, from https://www.asprs.org/wp/content/uploads/pers/2002journal/december/2002_dec.pdf

Region 6 PNW LiDAR Field Plot Procedures. (2019).

Riffell, S., Verschuyl, J., Miller, D., & Wigley, T. B. (2011). Biofuel harvests, coarse woody debris, and biodiversity - A meta-analysis. Forest Ecology and Management, **261**(4), 878–887. https://doi.org/10.1016/j.foreco.2010.12.021

Rondeux, J., Sanchez, C., Rondeux, J., & Sanchez, · C. (2010). Review of indicators and field methods for monitoring biodiversity within national forest inventories. Core variable: Deadwood. Environ Monit Assess, **164**, 617–630. https://doi.org/10.1007/s10661-009-0917-6

Roussel, J. R., Auty, D., Coops, N. C., Tompalski, P., Goodbody, T. R. H., Meador, A. S., Bourdon, J. F., de Boissieu, F., & Achim, A. (2020). lidR: An R package for analysis of Airborne Laser Scanning (ALS) data. Remote Sensing of Environment, 251. https://doi.org/10.1016/J.RSE.2020.112061

Seielstad, C. A., & Queen, L. P. (2003). Using airborne laser altimetry to determine fuel models estimating fire behavior. Journal of Forestry, **101**(4), 10–17. https://doi.org/10.1093/jof/101.4.10

Shokirov, S., Schaefer, M., Levick, S. R., Jucker, T., Borevitz, J., Abdurahmanov, I., & Youngentob, K. (2021). Multi-platform LiDAR approach for detecting coarse woody debris in a landscape with varied ground cover. International Journal of Remote Sensing, **42**(24), 9316–9342. https://doi.org/10.1080/01431161.2021.1995072

Sullivan, T. P., Sullivan, D. S., Lindgren, P. M. F., & Ransome, D. B. (2012). If we build habitat, will they come? Woody debris structures and conservation of forest mammals. Journal of Mammalogy, **93**(6), 1456–1468. https://doi.org/10.1644/11-MAMM-A-250.1

US Department of Agriculture Forest Service. (2022). Field instructions for the annual inventory

of Washington, Oregon and California. 384.

van Aardt, J. A. N., Arthur, M., Sovkoplas, G., Swetnam, T. L., & Aardt, J. van. (2011). LiDAR-based estimation of forest floor fuel loads using a novel distributional approach. SilviLaser 2011, 11th International Conference on LiDAR Applications for Assessing Forest Ecosystems, University of Tasmania, Australia, 1–8. http://www.locuscor.net/silvilaser2011/papers/063_van Aardt.pdf

White, J. C., Wulder, M. A., Varhola, A., Vastaranta, M., Coops, N. C., Cook, B. D., Pitt, D., & Woods, M. (2013). A best practices guide for generating forest inventory attributes from airborne laser scanning data using an area-based approach. Forestry Chronicle, **89**(6), 722–723. https://doi.org/10.5558/tfc2013-132

Windrim, L., Bryson, M., Mclean, M., Randle, J., & Stone, C. (2019). Remote sensing Automated Mapping of Woody Debris over Harvested Forest Plantations Using UAVs, High-Resolution Imagery, and Machine Learning. https://doi.org/10.3390/rs11060733

Woldendorp, G., Keenan, R. J., Barry, S., & Spencer, R. D. (2004). Analysis of sampling methods for coarse woody debris. Forest Ecology and Management, **198**(1–3), 133–148. https://doi.org/10.1016/j.foreco.2004.03.042

Zald, H. S. J., Ohmann, J. L., Roberts, H. M., Gregory, M. J., Henderson, E. B., McGaughey, R. J., & Braaten, J. (2014). Influence of lidar, Landsat imagery, disturbance history, plot location accuracy, and plot size on accuracy of imputation maps of forest composition and structure. Remote Sensing of Environment, **143**, 26–38. https://doi.org/10.1016/j.rse.2013.12.013

Zhang, K., Chen, S. C., Whitman, D., Shyu, M. L., Yan, J., & Zhang, C. (2003). A progressive morphological filter for removing nonground measurements from airborne LIDAR data. IEEE Transactions on Geoscience and Remote Sensing, 41(4 PART I), 872–882. https://doi.org/10.1109/TGRS.2003.810682

Zhang, W., Qi, J., Wan, P., Wang, H., Xie, D., Wang, X., & Yan, G. (2016). An Easy-to-Use Airborne LiDAR Data Filtering Method Based on Cloth Simulation. Remote Sensing 2016, Vol. 8, Page 501, **8**(6), 501. https://doi.org/10.3390/RS8060501